UNIVERSIDADE DO VALE DO RIO DOS SINOS - UNISINOS
UNIDADE ACADÊMICA DE PESQUISA E PÓS-GRADUAÇÃO
PROGRAMA DE PÓS-GRADUAÇÃO EM ENGENHARIA MECÂNICA
NÍVEL MESTRADO

RAFAEL FERNANDO DUTRA

CONSTRUCTAL DESIGN OF AN IDEALIZED ARTERIAL BYPASS GRAFT SUBJECTED TO NEWTONIAN AND NON-NEWTONIAN BLOOD FLOW

São Leopoldo
2020

RAFAEL FERNANDO DUTRA

CONSTRUCTAL DESIGN OF AN IDEALIZED ARTERIAL BYPASS GRAFT SUBJECTED TO NEWTONIAN AND NON-NEWTONIAN BLOOD FLOW

Dissertação apresentada como requisito parcial para obtenção do título de Mestre em Engenharia Mecânica, pelo Programa de Pós-Graduação em Engenharia Mecânica da Universidade do Vale do Rio dos Sinos – UNISINOS.

Orientadora: Prof.ª Dra. Flávia Schwarz Franceschini Zinani

Coorientador: Prof. Dr. Luiz Alberto Oliveira Rocha

São Leopoldo

2020

D978c Dutra, Rafael Fernando.
Constructal design of an idealized arterial bypass graft subjected to Newtonian and non-Newtonian blood flow / Rafael Fernando Dutra. – 2020.
71 f. : il. ; 30 cm.

Dissertação (mestrado) – Universidade do Vale do Rio dos Sinos, Programa de Pós-Graduação em Engenharia Mecânica, 2020.
"Orientadora: Prof.ª Dra. Flávia Schwarz Franceschini Zinani ; coorientador: Prof. Dr. Luiz Alberto Oliveira Rocha".

1. Constructal design. 2. Newtonian blood. 3. Non-Newtonian blood. 3. Carreau model. 4. Coronary artery bypass graft. 5. Dimensionless pressure drop. I. Título.
CDU 621

Dados Internacionais de Catalogação na Publicação (CIP)
(Bibliotecário: Flávio Nunes – CRB 10/1298)

RAFAEL FERNANDO DUTRA

CONSTRUCTAL DESIGN OF AN IDEALIZED ARTERIAL BYPASS GRAFT SUBJECTED TO NEWTONIAN AND NON-NEWTONIAN BLOOD FLOW

Dissertação apresentada como requisito parcial para obtenção do título de Mestre em Engenharia Mecânica, pelo Programa de Pós-Graduação em Engenharia Mecânica da Universidade do Vale do Rio dos Sinos – UNISINOS.

Aprovado em 06 de abril 2020.

BANCA EXAMINADORA

_____

Dr. Antonio Ferreira Miguel – Universidade de Évora

_____

Dra. Rejane de Césaro Oliveski – UNISINOS

_____

Dr. Paulo Roberto Wander – UNISINOS

ACKNOWLEDGEMENTS

This study was financed in part by the Coordenação de Aperfeiçoamento de Pessoal de Nível Superior - Brasil (CAPES) - Finance Code 001.

ABSTRACT

Abstract. Arterial bypass grafts tend to fail after some years due to Intimal Hyperplasia – an abnormal proliferation of smooth muscle cells that leads to restenosis and graft occlusion. In this regard and based on the Constructal Design method, this dissertation, that is presented in the form of two articles, seeks to investigate the effect of geometric parameters and the influence of Carreau rheological parameters on the flow through a bypass graft circumventing an idealized, partially-stenosed coronary artery. The computational model assumes steady-state fluid flow through an idealized model for a partially stenosed artery with a bypass graft. A Computational Fluid Dynamics model and a Response Surface Methodology were employed to assess the effects of bypass geometry on pressure drop. The first article presented the analysis for a Newtonian fluid. As the diameter ratio D_1/D increased and the junction angle α decreased, the pressure drop decreased and so the dependence of pressure drop on the stenosis degree. The effects of diameter ratio were more pronounced than those of junction angle on the velocity field and wall shear stress. The optimum point for all cases was $D_1/D_{,opt}$ equal to 1 and $\alpha_{,opt}$ equal to 30°, which is corroborated by previous studies. In a second article, the differences in between the Newtonian and non-Newtonian results were presented, through the analysis of the influence of rheological parameters of the Carreau model for blood. All the response surfaces generated for both the Newtonian and non-Newtonian cases presented a great similarity. The results obtained demonstrated that non-Newtonian rheological parameters did not influence neither the shape of the response surfaces nor the optimum points found, although they have a great impact on pressure drop, mainly the parameters η^* and n. Besides, it was also evaluated the effects on velocity and wall shear stress caused by the variation of rheological parameters, where, η^* and n, appear to have a more pronounced influence than λ. Finally, the results found in this dissertation demonstrated that the application of the Constructal Design method in hemodynamics might be a good alternative to provide configurations with enhanced performance and to provide valuable results to the understanding of biological flows.

Keywords: Constructal Design, Newtonian blood, non-Newtonian blood, Carreau model, coronary artery bypass graft, dimensionless pressure drop.

LIST OF FIGURES

LIST OF TABLES

NOMENCLATURE

D	artery diameter	[m]
D_0	stenosis diameter	[m]
D_1	graft diameter	[m]
D_{ij}	strain rate tensor	[s^{-1}]
$D_1/D_{,opt}$	optimum diameter ratio	[-]
L	Length	[m]
M	number of verification points	[-]
N	power law index	[-]
N	number of mesh elements	[-]
$\tilde{p}$	dimensionless pressure drop	[-]
$\tilde{p}_{min}$	minimum dimensionless pressure drop	[-]
$\tilde{p}_{obs}$	dimensionless pressure drop observed from verification points	[-]
$\tilde{p}_{pred}$	dimensionless pressure drop predicted from response surface	[-]
Re	Reynolds number	[-]
S	stenosis degree	[-]
U_m	average velocity	[m s^{-1}]
u_i	velocity vector	[m s^{-1}]
$\tilde{u}_i$	dimensionless velocity field	[-]
V	artery volume	[m^3]
V_1	graft volume	[m^3]
$\tilde{X}$	dimensionless position	[-]
X	position vector	[m]
$\tilde{x}_i$	dimensionless position vector	[-]

Greek symbols

α	junction angle	[-]
$\alpha_{,opt}$	optimum junction angle	[-]

Δp	pressure drop	[Pa]
η	viscosity function	[Pa s]
η_c	characteristic viscosity	[Pa s]
η_0	zero shear rate viscosity	[Pa s]
η_∞	infinite shear rate viscosity	[Pa s]
$\tilde{\eta}$	dimensionless viscosity function	[-]
η^*	dimensionless viscosity ratio	[-]
λ	time constant	[-]
$\tilde{\lambda}$	Carreau number	[-]
μ	dynamic viscosity	[Pa s]
ρ	mass density	[kg m^{-3}]
$\dot{\gamma}$	shear rate	[s^{-1}]
τ^*	normalized shear stress	[-]
τ_{ij}	extra-stress tensor	[Pa]
$\tilde{\tau}_{ij}$	dimensionless extra vector tensor field	[-]

SUMMARY

1 INTRODUCTION

Atherosclerosis is the main disease which affects large and medium arteries. It is characterized by the artery hardening and thickening caused by the accumulation of lipids, e.g., low density lipoproteins or LDL. According to Tian et al. (2013) and Liu et al. (2015) this abnormal accumulation, which causes obstruction to the blood circulation, is commonly designated as stenosis. It has already been proved that hemodynamic plays an important role in the localization of vascular disease in complex flow regions (e.g. carotid, aorta, and other proximal arteries). These areas of complex flows often occur in branching, bifurcations and artery curvatures (CHAICHANA et al., 2011; IASIELLO et al., 2017). However, Liu et al. (2015) stated that the understanding of the plaque development mechanism is still somewhat unclear, despite intensive investigations by many researchers. The low and/or oscillatory Wall Shear Stress (WSS) hypothesis proposed by Caro et al. (1971) and reaffirmed by Ku et al. (1985) has become the consensus mechanism for the initiation of atherosclerosis for most current investigations. This supposition assumed that plaques tend to initiate and develop in areas of low and oscillatory wall shear stress. However, as explained by Peiffer et al. (2013), some studies have found evidences that do not support such hypothesis, making the low WSS theory less robust than commonly assumed.

Coronary artery bypass graft (CABG) surgery is the standard treatment for coronary artery high-risk patients and consists in by-passing a stenotic region of a coronary artery in order to restore the proper blood flow to the heart (GUERCIOTTI et al., 2017). As reported by Bassiouny et al. (1992), the main factor that affects graft patency is intimal hyperplasia (IH), an abnormal proliferation of smooth muscle cells that is mainly observed between the graft and the coronary artery, resulting in the reduction of the lumen of the graft and leading to restenosis and graft occlusion. This type of vascular disease is hypothesised to be promoted by the presence of hemodynamic disturbances (e.g., stagnation and recirculation regions) and unnatural shear stimulation of the arterial wall, especially in the region of the anastomosis (OJHA et al., 1993; OJHA et al., 1994; HARUGUSHI et al., 2003). In this respect, Vimmr et al. (2012) and Fan et al. (2016) explained that multiple morphometric aspects, such as anastomotic configuration, severity of native coronary artery stenosis, blood rheology and CABG geometry, tend to influence the hemodynamics in the CABG and host arteries and play an important role in potential graft failure due to IH.

Several numerical studies in hemodynamics have investigated the occlusion causes and the use of the arterial graft as a definitive solution to the problem. Some authors used

three-dimensional numerical models to investigate the effects on Newtonian blood flow field caused by different locations of the stenosis (BERTOLOTTI and DEPLANO, 2000; KO et al., 2007), different Reynolds number (LEE et al., 2001; CHUA et al., 2005b), different graft diameter (FAN et al., 2016), different junction angles (LEE et al., 2001; KO et al., 2008), fluid deflector (ROOS et al., 2013) and compliance mismatch (POST et al., 2019). Other studies applied optimization methods to predict the best geometry of the graft according to the diameter of the artery and graft (CHUA et al., 2005a; XIONG and CHONG, 2008; DO et al., 2010; VIMMR et al., 2012), junction angle (XIONG and CHONG, 2008; DO et al., 2010; VIMMR et al., 2012) and stenosis degree (VIMMR et al., 2012). Different bypass geometries have also been simulated by some authors in an attempt to find a more suitable model. Figure (1.1) illustrates Taylor patch (LEI et al., 1997; COLE et al., 2002), Miller-cuff (LEUPRECHT et al., 2002), helical-graft (LIU et al., 2016), T-graft (POLITIS et al., 2007), Y-graft (LEI et al., 1997; COLE et al., 2002; POLITIS et al., 2007) and S-graft (FAN et al., 2008) which are some examples of what has already been researched in literature. All of these models were an attempt to mitigate the occurrence of Intimal Hyperplasia, however, none of them is considered as a definitive solution. Taylor patch (Fig. 1.1a) and Miller-cuff (Fig. 1.1b) cause a problem related to an extensive suture line, despite providing better hemodynamics in the bypass outlet. Each one of the other models listed in the Fig (1.1c to 1.1f) has better fit in the artery, but they did not permanently attenuate the presence of hemodynamic disturbances.

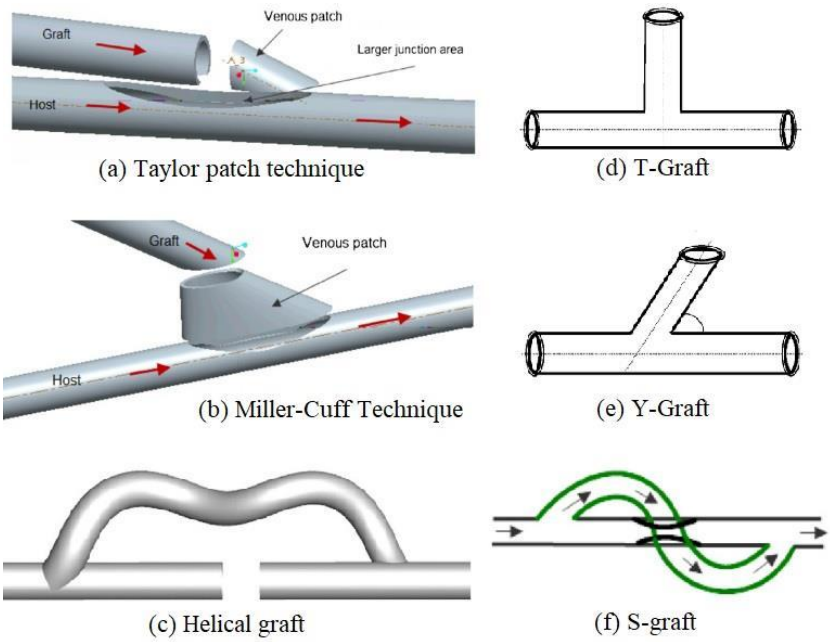

Figure 1.1 – Some examples of graft designs. (a) Taylor patch (OWIDA et al., 2012), (b) Miller-cuff (OWIDA et al., 2012), (c) helical-graft (LIU et al., 2016), (d) T-graft (POLITIS et al., 2007), (e) Y-graft (POLITIS et al., 2007) and (f) S-graft (FAN et al., 2008).

Blood is a suspension of red blood cells (RBC) and plasma with white blood cells and platelets in relatively low volume fractions (HORNER et al., 2018). According to Owens (2006), blood is essentially a non-Newtonian fluid, showing shear-thinning behaviour, and, additionally, both thixotropic and viscoelastic properties. Johnston et al. (2004) asserted that, despite the considerable amount of viscosity models, none of them fully expresses the effects of the extremely complicated nature of blood rheology. The blood properties are dependent on cell concentration, coagulation, adhesion and oxygen concentration and its viscosity varies with the hematocrit, which is the percentage of the total blood volume occupied by blood cells (PEREIRA et al., 2013). Given these circumstances, several authors have studied non-Newtonian blood behavior in the cardiovascular system, especially in stenotic arteries (RAZAVI et al., 2011; TIAN et al., 2013), branching (WEDDELL et al., 2015), bifurcations (KARIMI et al., 2014; APOSTOLIDIS et al., 2016; DOOST et al., 2016; IASIELLO et al., 2017) and curvature (JOHNSTON et al., 2004; JOHNSTON et al., 2006). However, fewer works focused their analysis in the non-Newtonian effects at arterial bypass grafts and their findings are not conclusive. While Chen et al. (2006) and O´Callaghan et al. (2006) demonstrated the importance of choosing a non-Newtonian model that can greatly influence velocity profiles and WSS, Vimmr and Jonásová (2010) and Vimmr et al. (2013) concluded that the non-Newtonian blood flow does not significantly differ from the Newtonian, because the relatively high values of shear rate led to mostly insignificant changes in the flow field.

The Constructal Law was stated by Adrian Bejan, J.A. Jones Professor of Mechanical Engineering at Duke University, in 1996 as follows: “For a finite-size system to persist in time (to live), it must evolve in such a way that it provides easier access to the imposed currents that flow through it” (BEJAN, 1997). The Constructal Law deals with the physical concepts of life, evolution, design, performance and time arrow (BEJAN, 2016). Under the Constructal Theory, evolution and design in nature are deterministic, because the living systems evolve in such a way to decrease resistance to flow (BEJAN and LORENTE, 2011). Constructal Design is the study and mathematical modeling of flow systems evolution. It has the objective to explain the configuration of existing systems in nature and to design flow systems in engineering. This design methodology has the objectives of accessing the effects of shape and geometry in flow performance and finding the optimal geometry according to the Constructal Law (ROCHA et al., 2017).

The growth of the scientific research concerning the Constructal Law has been documented in review articles (REIS, 2006; BEJAN and LORENTE, 2011; CHEN, 2012), books (BEJAN, 1997; BEJAN and LORENTE, 2008; BEJAN and ZANE, 2012; BEJAN,

2016), several independent websites (http://constructallaw.com; http://constructal.org; http://www.sciencedaily.com/terms/constructal_theory.htm; http://www.scoop.it/t/constructal-design) and eleven international Constructal Law Conferences (most recently in Porto Alegre, Brazil, 2019). The applications of the Constructal Design cover many engineering fields, such as heat and mass transfer, renewable energy, manufacture and materials.

Until now, the few applications of Constructal Design in medicine have concerned with the field of cancer treatments, as studied by Wang et al. (2007), where the crucial problem was to keep the temperature of the normal tissue surrounding the tumor below a certain threshold so as not to damage the tissue itself. In this regard, Lucia and Grisolia (2018) studied the entropy generation related to the pH changes obtained by the ions transport through a membrane, and related to mitosis/apoptosis ratio, fundamental to evaluate the probability of evolution of cancer. Other two works in vision area used an approach based on the Constructal Law to analyse the pressure inside the eyes anterior chamber in relation to the biomechanical properties of corneas (LUCIA et al., 2016) and verified how the chloride ions fluxes can determine the water inflow and outflow, understanding how intraocular pressure is controlled by these fluxes (LUCIA et al., 2017). Nevertheless, at the best of the author knowledge, none work applied Constructal Design to the design of blood flow devices, such as arterial bypass grafts.

In view of the above, this work intends to extend the application of the Constructal Theory to hemodynamics area, applying the Construtal Design method to investigate the geometry of bypass graft subjected to Newtonian and non-Newtonian flow.

1.1 DEFINITION OF THE THEME

The present work studies numerically the blood flow through a bypass graft circumventing a partially stenosed idealized coronary artery, analysing the effects of geometric and rheological parameters and searching for the best configurations that minimize pressure drop for different blood flow conditions.

1.2 OBJECTIVES

1.2.1 General Objectives

The general objective of the present work is to perform a numerical study of the blood flow in a bypass graft circumventing a partially stenosed idealized coronary artery, by

applying the Constructal Design to investigate the configurations with best performances and understand the role of fluid rheology on design performance.

1.2.2 Specific Objectives

The specific objectives of this work are:

a) Introduce Constructal Design in the hemodynamics area to collaborate with the arterial graft designs studies;
b) Analyze the combined and isolated effect of stenosis degree, diameter ratio and junction angle on pressure drop, velocity contours and wall shear stress (WSS) in different blood flow conditions;
c) Analyze the effects of rheological parameters of a shear-thinning fluid model for blood by applying the Carreau model, on pressure drop, velocity contours, wall shear stress (WSS), and on the optimal geometry bypass designs.

1.3 JUSTIFICATION

The work is justified by the open question related to the development of an optimal configuration that increases the graft patency rate and makes it a definitive solution. Another important point is the introduction of Constructal Design method in the area of hemodynamics, which may provide valuable results in the future for problems that literature still does not find a definitive clarification, as the studied case.

1.4 RESEARCH STRUCTURE

The present work consists of four chapters. The first one presents the main motivations and objectives.

Chapter 2 is the first article. It introduces Constructal Design in the hemodynamics area and investigates the effect of geometric parameters on the flow through a bypass graft circumventing a partially stenosed idealized coronary artery. This paper reviews the state of the art and presents the methodology, results, and conclusions for the first part of the dissertation. This article was submitted to the Heat Transfer Journal and published in February 2020 (DUTRA et al., 2020).

Chapter 3 is the second article (not submitted). It makes a comparison between the Newtonian and non-Newtonian results and analyzes the influence of each rheological parameters of the Carreau model for blood.

Chapter 4 summarizes the main results of the present work.

2 CONSTRUCTAL DESIGN OF AN ARTERIAL BYPASS GRAFT

Abstract. *Arterial bypass grafts tend to fail after some years due to Intimal Hyperplasia – an abnormal proliferation of smooth muscle cells that leads to restenosis and graft occlusion. In this regard and based on the Constructal Design method, this study seeks to investigate the effect of geometric parameters – stenosis degree, junction angle and diameter ratio on the flow through a bypass graft circumventing an idealized, partially-stenosed coronary artery. The computational model assumes a steady-state Newtonian fluid flow through an artery stenosis degree from 25% to 75%. A Computational Fluid Dynamics model and a Response Surface Methodology were employed to assess the effects of the project parameters on pressure drop. As diameter ratio increases to 1 and the junction angle decreases to 30º, the pressure drop decreases and there is a considerable dependence of pressure drop on the stenosis degree. The effects of diameter ratio are more pronounced than those of junction angle on the velocity field and wall shear stress. The application of the Constructal Design method in hemodynamics might be a good alternative to provide configurations with enhanced performance and to provide valuable results to the understanding of biological flows.*

Keywords: *Constructal Design, blood flow, coronary artery bypass graft, dimensionless pressure drop.*

2.1 INTRODUCTION

The accumulation of fat in arteries walls can block partly or completely the flow of blood as well as cause atherosclerosis, which consists of a stiffening of the walls of these vessels (KU et al., 1985). As explained by Tian et al. (2013) and Liu et al. (2015) this abnormal accumulation is commonly designated as stenosis. Patients under these conditions can lose quality of life due to the loss of oxygenation of organs, tissues or the brain and are at risk for heart attacks or strokes. According to Guerciotti et al. (2017), one type of palliative treatment for high-risk patients is the coronary artery bypass graft (CABG) surgery, which consists of bypassing a stenotic region in order to restore proper blood flow to the heart. The main factor that affects graft patency is intimal hyperplasia (IH) – an abnormal proliferation of smooth muscle cells that is mainly observed between the graft and the coronary artery,

resulting in the reduction of the lumen of the graft and leading to restenosis and graft occlusion (BASSIOUNY et al., 1992).

Over the last two decades, computational fluid dynamics (CFD) methods have been used to investigate a possible correlation between hemodynamics in CABGs and IH development and aid in the development of an optimal graft design. Lei et al. (1997) analyzed the distribution of wall shear stress gradients for conventional geometries and demonstrated that it was possible to design an optimal graft geometry that significantly reduced wall shear stress gradients. Bertolotti and Deplano (2000) used a three-dimensional numerical model with different locations of the stenosis relative to the downstream junction and concluded that the risks of intimal hyperplasia at the anastomosis might be reduced by increasing the distance between the stenosis and the junction. Lee et al. (2001) studied the flow behavior of a complete bypass graft and a 100% occluded artery with different Reynolds number and junction angles. They demonstrated that the entrance and the exit junctions of the bypass were the two critical locations where the flow became disordered generally with recirculation zones. Cole et al. (2002) performed numerical simulations in a specific modified geometry of the Taylor graft in a totally-occluded artery and discovered that this modification led to hemodynamic benefits preventing intimal hyperplasia. Leuprecht et al. (2002) investigated the influence on the hemodynamic behavior and wall stresses caused by geometric conditions and different compliance of a conventional graft and the Miller-cuff type graft. Their results led to the conclusion that the better patency of the Miller-cuff prosthesis could be due to its larger space, demonstrating the considerable influence of asymmetries and local geometric irregularities on flow pattern. Chua et al. (2005a) investigated sleeve models that exhibited optimized hemodynamics flows to be used as mechanical connectors between the bypass graft and host artery at the distal anastomosis, eliminating the need for quality suturing. Three models were studied varying the diameter and height of the sleeves and it was concluded that the sleeve model, which had the same diameter of the artery and the graft, exhibited improving hemodynamics flow characteristics . In a second study, Chua et al. (2005b) studied the flow characteristics of a complete coronary artery bypass graft (CABG) connecting two different arteries, the Aorta and the coronary artery, and found that smaller grafting angle and smooth geometry reduced the high wall shear stress gradient in junctions, thereby improving the long-term graft patency rate. Politis et al. (2007) compared simulated blood flow in four different configurations of simplified composite arterial coronary grafts and suggested that the Y- and T-grafts were the best cases in terms of hemodynamic performance. Ko et al. (2007) performed simulations in a stenosed artery with a complete bypass graft to verify the

influence in flow fields of different severity of occlusions (0%, 70%, 80%, 90%, and 100% area stenosis) in a fixed junction angle and graft diameter. They pointed out the influences of stenosis severity on the flow fields and suggested that this could be one of the causes of restenosis in the host artery with bypass graft implantation. Fan et al. (2008) studied numerically and experimentally the hemodynamics effects of an S-type bypass, demonstrating the occurrence of a swirling flow that altered the overall flow pattern and eliminated the low WSS zone along the host artery floor. Ko et al. (2008) compared the effects on the flow field of three different junction angles (45º, 60º and 75º) in a 70% area-occluded artery with a complete bypass graft and concluded that flow features (e.g., recirculation, secondary flow and WSS distribution) in the stenosed host artery and the bypass graft were closely related with the junction angle. Xiong and Chong (2008) and Do et al. (2010) investigated numerically the diameter ratio and the angle between the graft and host artery and both suggested that a higher diameter and a junction angle between 30º to 45º would enhance long-term performance and lessen the development of IH. Vimmr et al. (2012) performed several numerical simulations of a complete three-dimensional coronary bypass model as a function of three geometrical parameters (stenosis degree, junction angle, and diameter ratio) and discovered that the diameter ratio was the most crucial parameter for coronary artery bypass grafting (CABG). Roos et al. (2013) focused their graft study in the illustration of potential benefits from the introduction of a fluid deflector to prevent the suture line from unhealthily high wall shear stress results. Their results suggested that a fluid deflector may be useful and beneficial in increasing the patency of the optimized graft. Fan et al. (2016) numerically studied the distribution of hemodynamic parameters in the left internal mammary artery (LIMA) bypass graft with stenosis of different degrees at various periods after surgical revascularization postoperative. It was discovered that hemodynamics were associated with multiple morphometric parameters; i.e., graft configuration, severity of stenosis and LIMA geometry. Liu et al. (2016) numerically investigated the effectiveness of helical arterial grafts by comparing the hemodynamic performance of conventional and this kind of graft with different positions and smooth tapers. Their findings suggested that the new helical graft with taper would significantly enhance helical flow, which would reduce the thrombus formation and IH. Post et al. (2019) focused their analysis to estimate changes in fluid flow and wall shear stress as a function of graft compliance with the host artery and concluded that high compliance grafts displayed minimal changes in fluid flow and arterial remodeling.

According to Constructal Law, stated by Adrian Bejan in 1996, “for a finite-size flow system to persist in time (to live) it must evolve with freedom in such a way that it provides

easier access to imposed currents that flow through it" (BEJAN, 1997). Constructal Law deals with the physical concepts of life, evolution, design, performance and time arrow (BEJAN, 2016). Under Constructal Theory, evolution and design in nature are deterministic because the living systems evolve in such a way to decrease resistance to flow (BEJAN and LORENTE, 2011). The growth of scientific research concerning Constructal Law has been documented in review articles (REIS, 2006; BEJAN and LORENTE, 2011; CHEN, 2012) and books (BEJAN, 1997; BEJAN and LORENTE, 2008; BEJAN and ZANE, 2012; BEJAN, 2016).

Constructal Design is the study and mathematical modeling of flow systems evolution. It has the capability to explain the configuration of existing systems in nature and to design flow systems in engineering. This design methodology has the objectives of accessing the effects of shape and geometry in flow performance and finding the optimal geometry according to Constructal Law (ROCHA et al., 2017). The applications of Constructal Design cover many engineering fields such as heat and mass transfer, renewable energy, manufacture and materials (ROCHA et al., 2017; RAZERA et al., 2018; FAGUNDES et al., 2019). Until now the few applications of Constructal Theory in medicine were within the field of cancer treatments, as studied by Wang et al. (2007) and Lucia and Grisolia (2018), and vision, in two papers by Lucia et al. (2016) and Lucia et al. (2017).

Based on the Constructal Design method, this study seeks to investigate the effect of geometric parameters on the flow through a bypass graft circumventing an idealized, partially-stenosed coronary artery. To this end, a Computational Fluid Dynamics model and Design of Experiments and Response Surface methodologies were used to evaluate the effect of geometric parameters on pressure drop in different flow conditions. To the best of the author knowledge, the present study is the first one to apply the Constructal Design method in hemodynamics to investigate blood flow devices. The introduction of the Constructal Design method to the field of hemodynamics brings a valuable tool to the understanding of biological problems since the bypass geometry is known to affect the blood flow field significantly and to play an important role in potential graft failure due to intimal hyperplasia.

2.2 METHODOLOGY

2.2.1 Constructal Design

The problem domain is shown in Fig. (2.1). It is an idealized version of an artery partially obstructed by fatty material deposition and implanted with a graft with both proximal

and distal anastomoses. The artery is represented as the host artery with a diameter equal to D and length equal to L. The main tube undergoes a stenosis that reduces it to diameter D_0. The geometry is symmetric over the center of the stenosis in the axial direction. The graft is placed at a distance L_2 from the center of the stenosis and its diameter is denoted D_1. The junction angle is α and the graft diameter is denoted D_1. L_3 is the distance from the center where the stenosis begins. The detailed locations of heel, toe, bed, inner-, outer-, and side-walls are indicated in Fig. (2.1).

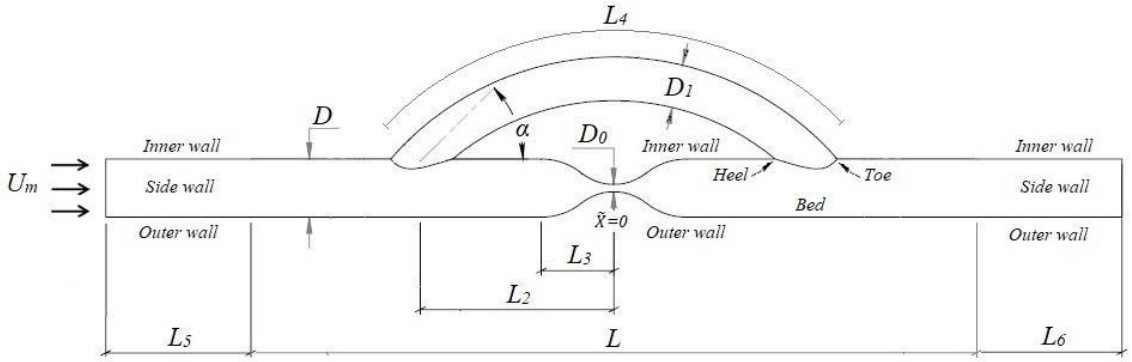

Figure 2.1 – Representation of the problem domain.

The flow problem consists of a fluid which enters the domain at the tube inlet with average velocity U_m. Depending on flow conditions and geometry configuration, the flow is partially deviated through the bypass. It is assumed that the tube walls are rigid, impermeable and non-slip. The flow is also assumed to be three-dimensional, steady, incompressible and laminar.

The full computational model for the geometry is depicted in Fig. (2.1) with main tube extensions of 25 diameters upstream and downstream (L_5=25.D and L_6=25.D) to obtain a fully developed flow. A uniform velocity profile, equal to U_m, was imposed at the inlet. At the outlet, a pressure outlet was imposed as boundary condition. For all simulations, the host artery diameter D is equal to 3 mm, corresponding to an average value of the right coronary artery (BERTOLOTTI et al., 2001).

Since the stenosis is usually formed by material deposition, the main tube volume is considered as its external volume was not narrowed:

$$V = \pi \frac{D^2}{4} L \tag{2.1}$$

where V is the total artery volume, D is the artery diameter and L is the total artery length.

The graft volume is

$$V_1 = \pi \frac{{D_1}^2}{4} L_4 \tag{2.2}$$

where V_1 is the total graft volume, D_1 is the graft diameter and L_4 is the total graft length.

The stenosis degree is calculated as

$$S = \frac{D - D_0}{D} x100\% \tag{2.3}$$

where S is the stenosis degree and D_0 is the diameter at the center of the stenosis.

The ratios L/D, L_2/D and L_3/D were defined as constants as detailed in Tab. (2.1). A baseline case from literature (VIMMR et al., 2012) was used in the definition of these values.

Table 2.1 – Geometric parameters for artery and graft build up.

Parameters	Values
L/D	16.67
L_2/D	2.5
L_3/D	1

Three values of stenosis degree S (25%, 50% and 75%) were evaluated at three different Reynolds Number, (150, 250 and 400). Blood is modelled as an incompressible Newtonian fluid with density $\rho = 1000\ \mathrm{kg/m^3}$ and dynamic viscosity $\mu = 0.0035$ Pa. s (KO et al., 2007). The assumption of blood as Newtonian fluid is acceptable and used by other studies in the hemodynamic area, e.g., Ko et al. (2007), Ko et al. (2008), Xiong, and Chong (2008) and Vimmr et al. (2012).

Constructal Theory assumes that living systems evolve limited by space (ROCHA et al., 2017). Accordingly, Constructal Theory systems must evolve in order to provide easier access to its flows (BEJAN and LORENTE, 2008). To this end, it was considered that the dimensionless pressure drop $\tilde{p}$ along the length L should be as low as possible.

Thus, an optimization problem was formulated as: “Find the minimum $\tilde{p}$. The design variables are the diameter ratio D_1/D and the junction angle α. The restrictions are constant L/D, L_2/D and L_3/D.” Therefore, the degrees of freedom for this problem are the diameter ratio D_1/D and the junction angle α. A search is conducted for the diameter ratio D_1/D and junction angle α that minimize the value of the pressure drop $\tilde{p}_{min}$ for specific combinations of S and Reynolds Number Re. To corroborate the results that minimize pressure drop, the

effect of the geometric variation on velocity contours and wall shear stress (WSS) arisen in the host artery are also analyzed. Figure (2.2) details all the steps required by the Constructal Design methodology.

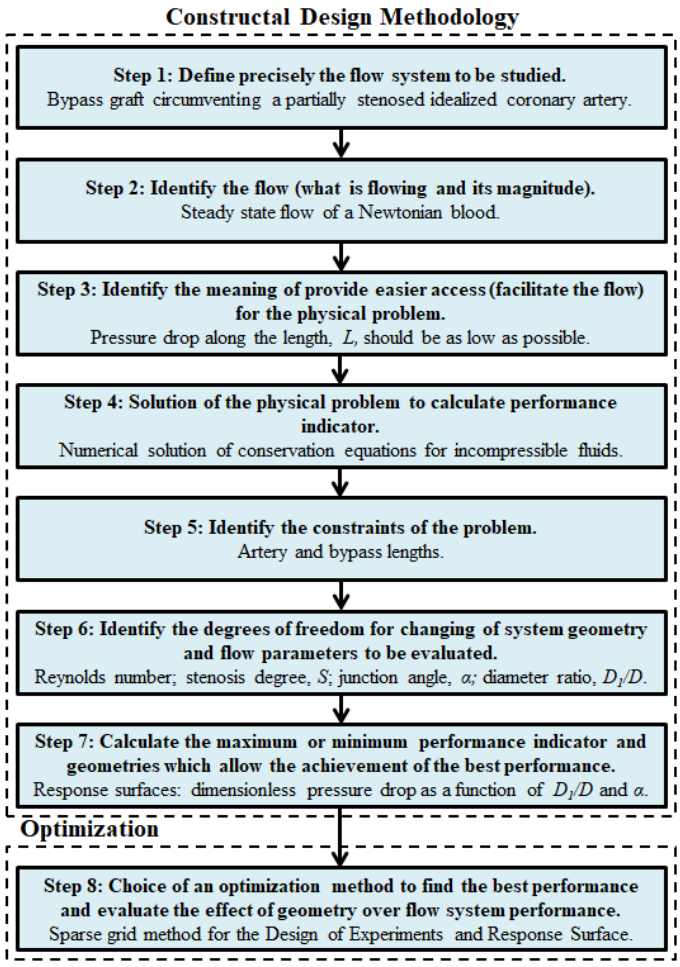

Figure 2.2 – Flowchart with application of Constructal Design and Sparse Grid methods for the present problem.

2.2.2 Mathematical Modeling

The mathematical modeling for the flow through the artery and bypass model consists of the mass and momentum balance equations for incompressible fluids. It is written these equations in their dimensionless form as follows:

$$\frac{\partial \tilde{u}_i}{\partial \tilde{x}_i} = 0 \tag{2.4}$$

$$\tilde{u}_i \frac{\partial \tilde{u}_i}{\partial \tilde{x}_j} = -\frac{\partial \tilde{p}}{\partial \tilde{x}_i} + \frac{1}{Re}\frac{\partial \tilde{\tau}_{ij}}{\partial x_j} \tag{2.5}$$

where $\tilde{u}_i$ denotes the dimensionless velocity field, $\tilde{x}_i$ the dimensionless position vector, $\tilde{p}$ the dimensionless pressure drop, $\tilde{\tau}_{ij}$ the dimensionless extra stress tensor field, Re the Reynolds number such that:

$$\tilde{u}_i = \frac{u_i}{U_m}; \qquad \tilde{x}_i = \frac{x}{D}; \qquad \tilde{p} = \frac{\Delta p}{\rho {U_m}^2}; \qquad \tilde{\tau} = \frac{\tau_{ij}}{(U_m \mu)/D} \qquad Re = \frac{\rho U_m D}{\mu} \qquad (2.6)$$

where Δp is the pressure drop along L, ρ is the fluid mass density and μ is the fluid viscosity and U_m is the average velocity at the inlet.

The constitutive equation for the extra stress is that of a generalized Newtonian liquid:

$$\tau_{ij} = 2\eta(\dot{\gamma})D_{ij} \qquad (2.7)$$

where $\eta(\dot{\gamma})$ is the viscosity function and D_{ij} is the strain rate tensor, given as the symmetric part of the velocity gradient tensor (SLATTERY, 1999). For a Newtonian fluid, $\eta(\dot{\gamma})$ is a constant and equal to μ.

2.2.3 Numerical Method and Computational Grid

In order to solve the system of partial differential equations, it was employed the Finite Volume Method (PATANKAR, 1980) using the ANSYS/FLUENT v. 18.2 (ANSYS, 2015). A pressure-based solver was used with a pressure-velocity coupling method and second-order interpolation functions for pressure and velocity fields. All calculations were conducted in double-precision representation of real numbers. The iterative algorithm was a false transient. The mesh was parameterized to keep proportional the element sizes according to the stenosis configuration and diameter ratio studied. Depending on the configuration, a total of 500,000 to 950,000 tetrahedral finite elements were necessary to mesh the computational domain accurately. Along the walls, prismatic layers elements were used in order to better capture the boundary layer. Figure (2.3) presents a sample of the computational mesh for the model with detailed views at the cross section in the bypass and native stenotic artery. As convergence criterion, scaled residuals of each equation at an iteration were used and compared with a user-defined convergence criteria equal to 10^{-6} for velocity and pressure fields.

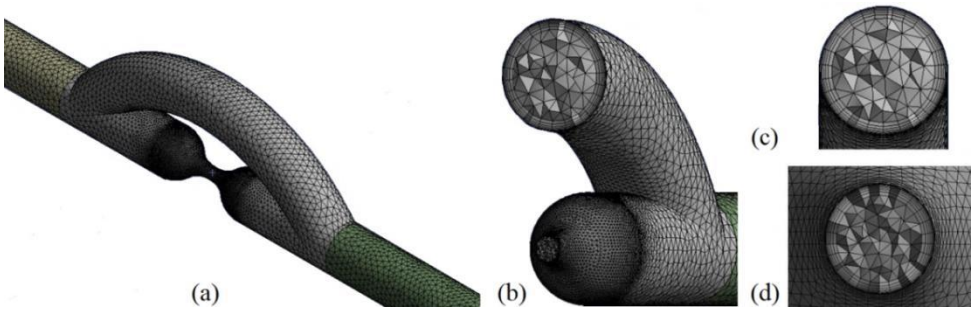

Figure 2.3 – Isometric view of the computational mesh for the model (a) with a detailed view at the cross section in the bypass and native stenotic artery (b) and a front mesh view of the bypass (c) and stenosis region (d).

The *Grid Convergence Index (GCI)* method was applied for different values of junction angle α and diameter ratio D_1/D in the three values of stenosis degree (S = 25%, 50%, and 75%). As explained by Celik et al. (2008), this method is useful for calculation and reporting of discretization error estimates in CFD simulations where experimental data may not be available for comparison. Table (2.2) summarizes these results where N represents the number of elements. It can be verified that the maximum *GCI* was 1.82%, refining the mesh in a factor of 15% to 30%. It is important to observe that, based on experience and not on formal derivation, a maximum GCI value of 5% is considered acceptable for this method (CELIK et al., 2008).

Table 2.2 – Some samples of *Grid Convergence Index (GCI)* for different bypass configurations at *Re = 250*.

	Case 1	Case 2	Case 3	Case 4	Case 5	Case 6	Case 7	Case 8
D_1/D	0,1	0,1	0,1	0,55	1	1	1	1
α	30°	30°	70°	50°	30°	30°	70°	70°
S	25%	75%	75%	50%	25%	75%	25%	75%
$N1$	529,773	820,701	669,261	731,031	640,062	940,363	510,872	803,049
$N2$	431,466	709,991	570,235	564,503	533,546	786,550	434,428	651,633
$N3$	364,651	542,664	454,099	425,013	455,450	574,455	368,760	490,328
$\tilde{p}_{,N1}$	2.712	133.408	133.475	4.796	2.258	2.659	2.362	3.924
$\tilde{p}_{,N2}$	2.715	133.493	133.874	4.835	2.326	2.662	2.415	3.928
$\tilde{p}_{,N3}$	2.723	136.925	134.216	4.847	2.331	2.676	2.437	3.929
GCI	**0.24%**	**0.10%**	**0.71%**	**0.42%**	**1.44%**	**0.55%**	**1.82%**	**1.66%**

2.2.4 Design of Experiments and Response Surface Methodology

To investigate the effects of the junction angle α and the artery diameter ratio D_1/D on the pressure drop along the length L, the Response Surface methodology available in ANSYS Design Xplorer 18.2 was applied (ANSYS, 2016). A sparse grid method (MONTGOMERY,

2013) was employed for the design of experiments to build the response surfaces and represent $\tilde{p}$ as a function of the degrees of freedom D_1/D and α, within the ranges $0.1 \leq D_1/D \leq 1.0$ and $30^o \leq \alpha \leq 70^o$. Sparse Grid is an adaptive model driven by the accuracy defined by the user. Initially, the program calculated four design points located at the edges and one design point located at the center of the response surface. Then, the response surface was elaborated with a maximum number of 1,000 design points per surface. This method increases the accuracy of the response surface by automatically refining the matrix of design points in locations where the relative error of the output parameter is higher, i.e., it refines design points only in the directions necessary (ANSYS, 2016). Figure (2.4) illustrates a response surface example with a different matrix of design points. It is noteworthy that each design point represents a specific bypass configuration within the ranges $0.1 \leq D_1/D \leq 1.0$ and $30^o \leq \alpha \leq 70^o$. In this study, the number of points needed to construct each surface ranged from 200 to 300.

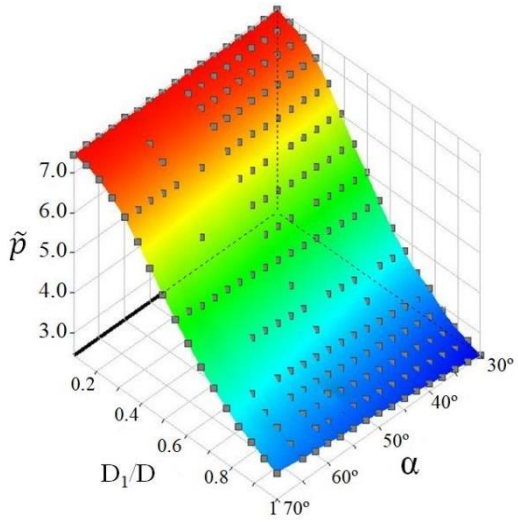

Figure 2.4 – Representation of a response surface with different matrix of design points generated by the Sparse Grid method.

After building the response surfaces, the method suggests verification points. It was performed ten verification points (individual simulations) for each response surface. Here the root mean square error (RMSE) was employed as an indicator of the quality of the response surface. The RMSE is defined as

$$RMSE = \sqrt{\frac{1}{m}\sum_{i=1}^{m}\left(\frac{\tilde{p}_{pred,i} - \tilde{p}_{obs,i}}{\tilde{p}_{obs,i}}\right)^2} x100 \qquad (2.8)$$

where $\tilde{p}_{pred}$ is the value of $\tilde{p}$ predicted from response surface, $\tilde{p}_{obs}$ is the value of $\tilde{p}$ observed from the verification points, and m is the number of verification points.

In all cases, there was a good agreement between individual simulations and the response surfaces. The maximum RMSE for the response surfaces presented in this work was of 1.33%.

2.3 RESULTS AND DISCUSSION

2.3.1 Model Verification

Preliminary tests were performed using the numerical model and their results for the wall shear stress (WSS) were compared with those of Ko et al. (2007) for the case of Reynolds number *Re* equal to 250, blood viscosity μ equal to 0.0035 Pa.s, blood density ρ equal to 1000 kg/m³ and the parameters of the arterial graft D_1/D equal to 1, junction angle α equal to 45° and stenosis degree *S* equal to 70%.The shear stress found at each point was normalized by the shear stress of a fully developed condition in the host artery. Three positions were verified on the wall artery (inner, outer and side wall, as presented in Fig. (2.1)).

Figure (2.5) presents the results of the verification for the inner wall and outer wall. The side wall results are not included for simplicity since they were similar to the outer wall results. It can be verified that for most points there was good agreement between the present results and literature.

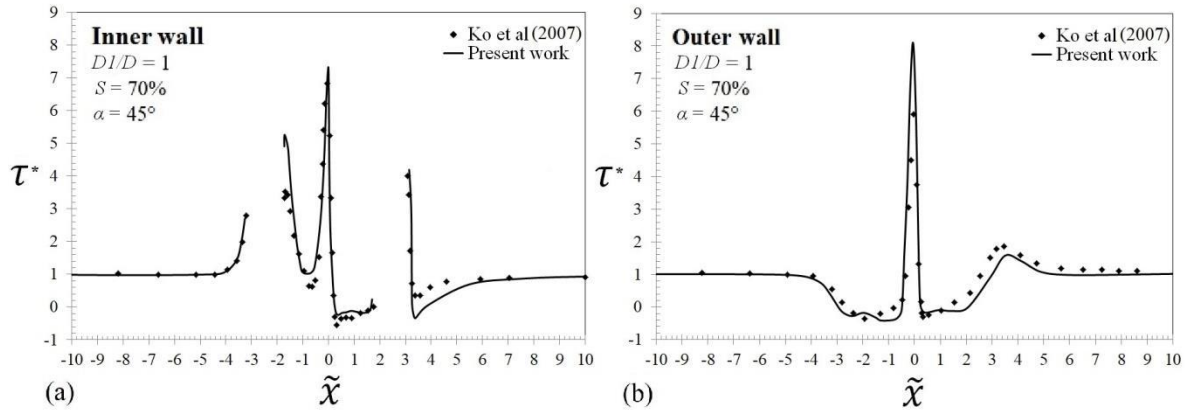

Figure 2.5 – Model verification. Results of the normalized shear stress, τ^*, on the inner wall (a) and outer wall (b).

2.3.2 Response Surfaces

Figure (2.6) shows the response surfaces that represent $\tilde{p}$ as a function of the degrees of freedom, D_1/D and α, within the ranges $0.1 \leq D_1/D \leq 1.0$ and $30^o \leq \alpha \leq 70^o$. Each response surface represents the results of stenosis degree S equal to 25%, 50% and 75% at Reynolds Number Re equal to 150, 250 and 400.

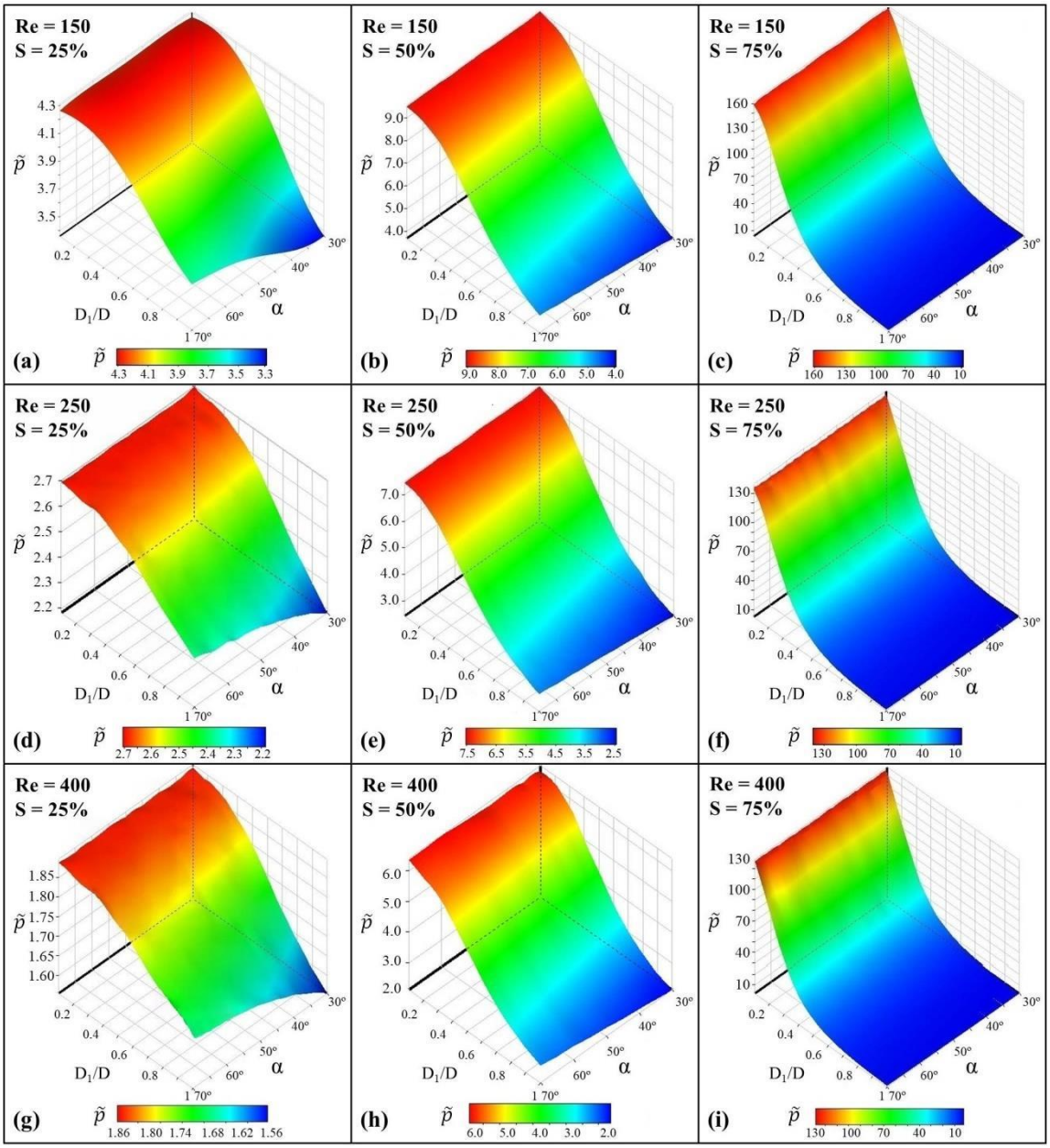

Figure 2.6 – Response surfaces representing $\tilde{p}$ as a function of D_1/D and α for the stenosis degree and Reynolds number as follow: (a) Re=150 / S=25%; (b) Re=150 / S=50%; (c) Re=150 / S=75%; (d) Re=250 / S=25%; (e) Re=250 / S=50%; (f) Re=250 / S=75%; (g) Re=400 / S=25%; (h) Re=400 / S=50%; (i) Re=400 / S=75%.

It is possible to observe that the nine response surfaces had a specific optimal point that minimized the dimensionless pressure drop $\tilde{p}$. For each case, a value of D_1/D and α where $\tilde{p}$ is minimum was obtained. In all situations, as the aspect ratio D_1/D increased to 1 and the junction angle, α, decreased to 30º, $\tilde{p}$ decreased. However, as the stenosis degree became larger, i.e. the flow highly deviated through the bypass and the influence of α in $\tilde{p}$ became almost unnoticeable. These results showed that the diameter ratio D_1/D had a more significant effect on the pressure drop than α. The prominent influence of the D_1/D ratio compared to the α angle had been confirmed experimentally (TSUKUI et al., 2017) and numerically (XIONG and CHONG, 2008; DO et al., 2010; VIMMR et al., 2012) in idealized steady and pulsatile stenotic flows. Tsukui et al. (2017) also confirmed that a smaller junction angle (α) yielded lower energy loss at bypass graft.

Table (2.3) summarizes the optimal geometry results for the nine configurations. It is possible to notice a considerable dependence of $\tilde{p}$ on the stenosis degree *S*. Also, the optimum point for all cases was $D_1/D_{,opt}$ equal to 1 and $\alpha_{,opt}$ equal to 30°. This result indicated that by increasing the aspect ratio D_1/D and decreasing the angle α a better result would be obtained. However, this situation would be impractical from the surgical standpoint because a graft of difficult suture would be produced (VIMMR et al., 2012). As a possible solution to this problem, Chua et al. (2005a) proposed sleeve models that could be used as mechanical connectors between the bypass graft and host artery, eliminating the need for quality suturing.

Table 2.3 – Optimum results for each stenosis degree, at *Re* equal to 150, 250 and 400.

Re	*S*	$\tilde{p}_{,min}$	$D_1/D_{,opt}$	$\alpha_{,opt}$
150	25%	3.315	1	30°
150	50%	3.685	1	30°
150	75%	3.978	1	30°
250	25%	2.186	1	30°
250	50%	2.435	1	30°
250	75%	2.659	1	30°
400	25%	1.574	1	30°
400	50%	1.755	1	30°
400	75%	1.942	1	30°

As according to Constructal Law, everything that flows generates forms and structures over time in order to facilitate its movement through mediums that offer resistances to the

flow (BEJAN and ZANE, 2012). So, by applying Constructal Design methodology, the optimum points found here were in accordance with previous studies that evaluated the graft design with other methodologies. Xiong and Chong (2008) speculated that a graft with a diameter ratio in the range of 1–1.5 larger than that of the host artery, and a junction angle in the range of 30°–45° would improve hemodynamics. Do et al. (2010) found a similar result, where the junction angle is 40º with a diameter ratio equal to 1.6. On the other hand, Vimmr et al. (2012) concluded that the most favorable flow field was observed for the bypass model with a diameter ratio equal to 1 while reducing the probability of bypass failure due to thrombosis or intimal hyperplasia.

2.3.3 Velocity Fields

Velocity field data is presented at *Re* equal to 250 and for *S* equal to 25%, 50%, and 75% to corroborate the results found on the response surfaces for the optimal bypass geometry. The main focus was on the isolated effect caused by the variation of the diameter ratio D_1/D and junction angle α. For each stenosis degree, velocity contours are shown in Fig. (2.7), (2.8) and (2.9) at different diameter ratios (D_1/D equal to 0.5; 0.7; and 1.0) for a fixed junction angle, equal to 30° ($\alpha_{,opt}$ found in Tab. (2.3)).

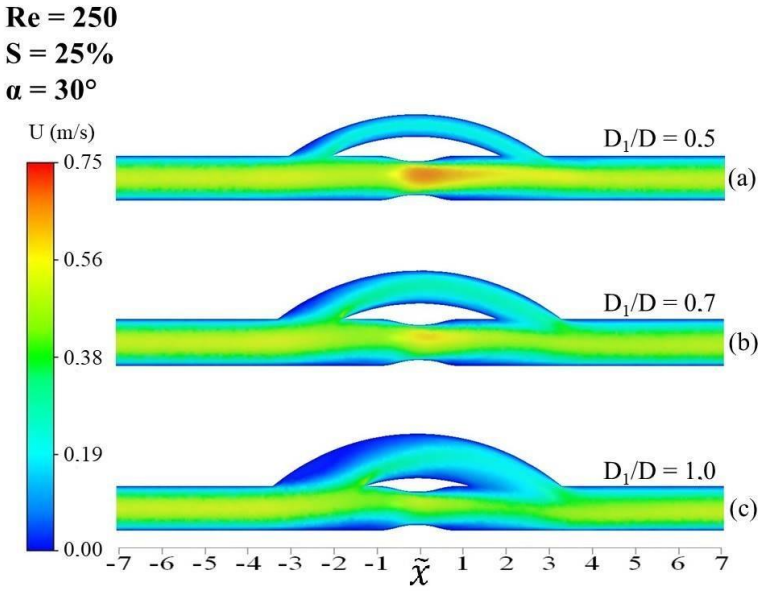

Figure 2.7 – Effect provided by the variation of diameter ratio, D_1/D, in a fixed junction angle, $\alpha_{,opt}$ = 30°, at velocity contours for stenosis degree, S = 25% and Re = 250. (a) D_1/D = 0.5; (b) D_1/D = 0.7; (c) D_1/D = 1.0.

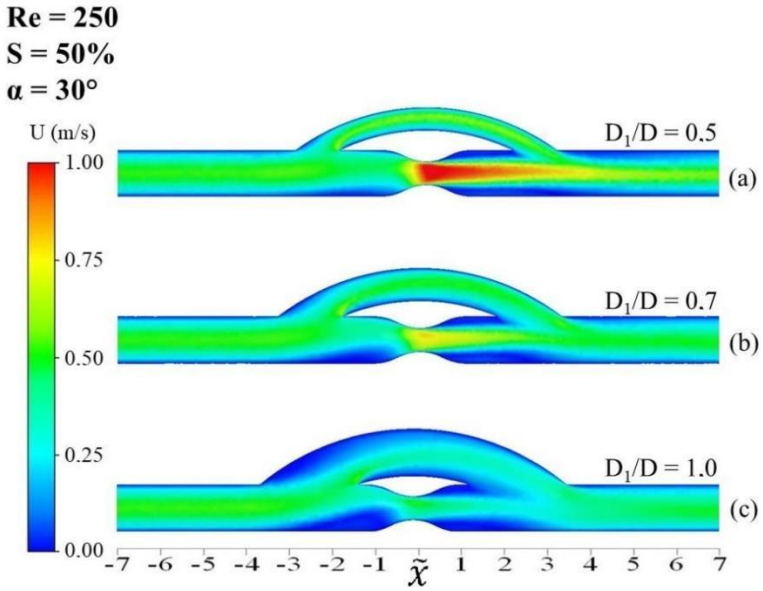

Figure 2.8 – Effect provided by the variation of diameter ratio, D_1/D, in a fixed junction angle, $\alpha_{,opt}$ = 30°, at velocity contours for stenosis degree, S = 50% and Re = 250. (a) D_1/D = 0.5; (b) D_1/D = 0.7; (c) D_1/D = 1.0.

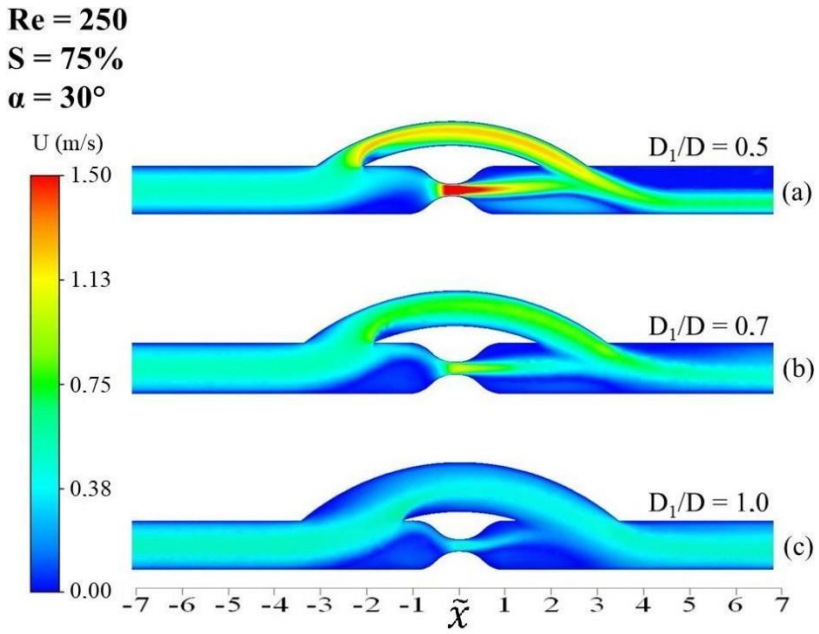

Figure 2.9 – Effect provided by the variation of diameter ratio, D_1/D, in a fixed junction angle, $\alpha_{,opt}$ = 30°, at velocity contours for stenosis degree, S = 75% and Re = 250. (a) D_1/D = 0.5; (b) D_1/D = 0.7; (c) D_1/D = 1.0.

As expected from section 2.3.2, the increase of aspect ratio D_1/D provided a greater flow deviation through the bypass. It is worth noting that for S equal to 25% the placement of the bypass graft did not significantly affect blood flow. As the degree of stenosis increased, the use of the bypass became more effective. These findings were consistent with Ko et al. (2007) and Vimmr et al. (2012), who asserted that stenosis degree smaller than 50% were

commonly described as hemodynamically insignificant because there was no impact on the blood supply to downstream tissues. Furthermore, according to Fan et al. (2016) a less severe stenosis could induce a small pressure gradient from the inlet of a bypass, causing a competitive flow through it and reducing its long term patency.

In addition, with the increase of D_1/D, larger recirculation zones appeared for stenosis of 50% ($\tilde{x}$ = -2 to 0 and $\tilde{x}$ = 1 to 3) and 75% ($\tilde{x}$ = -2 to 0 and $\tilde{x}$ = 1 to 3). This situation was already well reported by several authors. Bertolotti et al. (2001) and Ko et al. (2007) observed the recirculation zone upstream of the junction and pointed out that, downstream of the junction, the greater the bypass flow (i.e., as the stenosed severity increases), the greater the distance to obtain the maximum velocity at the center of the artery and the greater the distributing areas of recirculation zones. Lee et al. (2001) concluded that the entrance and the exit junctions of the bypass were the two critical locations where the curved, twisted and disturbed flow in the bypass was prone to damage the particles in the blood flow. Hence, recirculation zones next to the occlusion allow the damaged particles and substances to accumulate. Because of this phenomenon bypass surgery tends to fail after some years, being well recognized that non-uniform hemodynamics contributes to restenosis and the risk of thrombosis due to the possibility of blood cell accumulation (OWIDA et al., 2012; VIMMR et al., 2012).

Jet blood flow was observed in the post stenotic region ($\tilde{x}$ = 0), especially at severe degrees of stenosis (S = 75%) and when D_1/D had lower values. The complexity of these flow patterns had been analyzed in the most recent studies in the hemodynamic area at stenotic arteries without bypass graft. Conti et al. (2016), Sood et al. (2018) and Andersson et al. (2019) reported in their studies that such crossing pattern of the jet could impair essential endothelial functions and increase the susceptibility and progression of vascular diseases. The greater the degree of stenosis, the more distinct, stronger and eccentric was the jet flow. However, its role as a pathological determinant was still less understood (ANDERSSON et al., 2019).

Referring now to Fig. (2.10), (2.11) and (2.12), velocity contours are presented at different junction angles (α equal to 30º; 40º; 50º; 60º; and 70º) for a fixed diameter ratio equal to 1 ($D_1/D_{,opt}$ found in Tab. (2.3)).

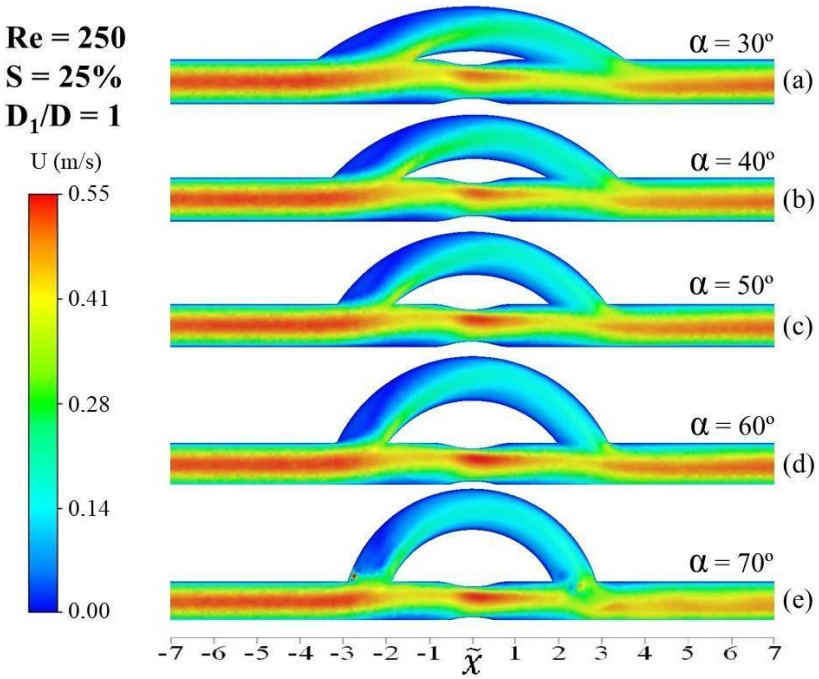

Figure 2.10 – Effect provided by the variation of junction angle, α, in a fixed diameter ratio, $D_1/D_{,opt} = 1$, at velocity contours for stenosis degree, $S = 25\%$ and $Re = 250$. (a) $\alpha = 30°$; (b) $\alpha = 40°$; (c) $\alpha = 50°$; (d) $\alpha = 60°$; (e) $\alpha = 70°$.

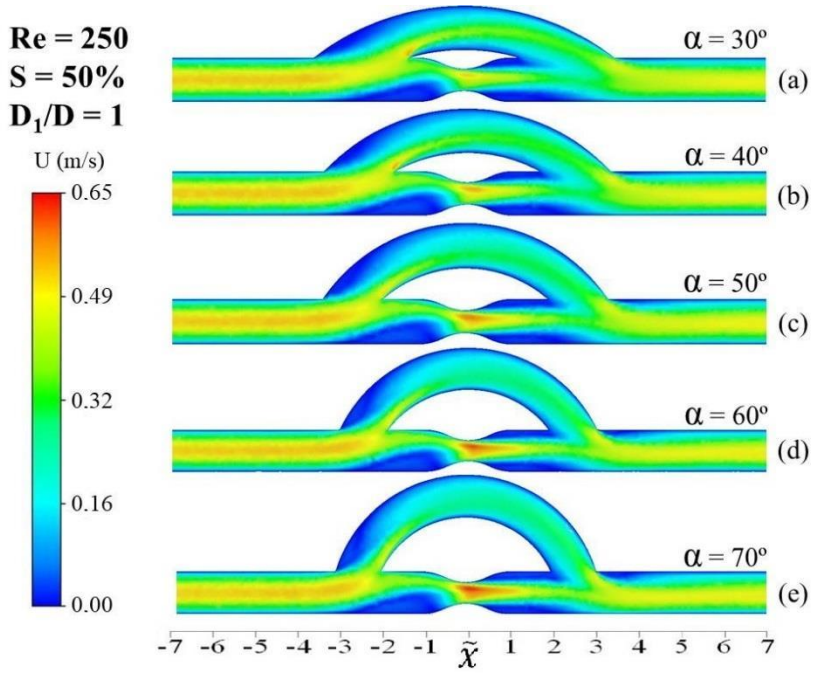

Figure 2.11 – Effect provided by the variation of junction angle, α, in a fixed diameter ratio, $D_1/D_{,opt} = 1$, at velocity contours for stenosis degree, $S = 50\%$ and $Re = 250$. (a) $\alpha = 30°$; (b) $\alpha = 40°$; (c) $\alpha = 50°$; (d) $\alpha = 60°$; (e) $\alpha = 70°$.

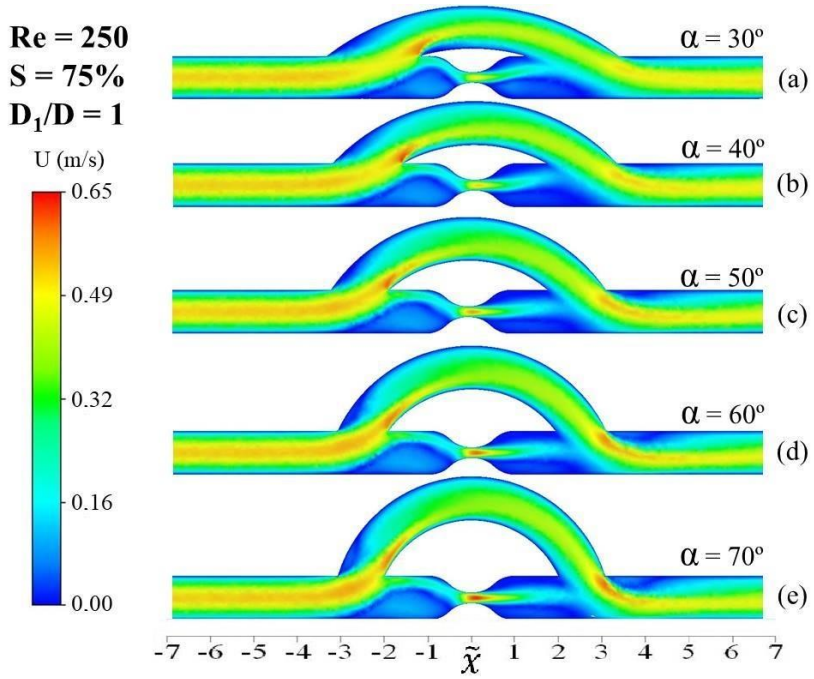

Figure 2.12 – Effect provided by the variation of junction angle, α, in a fixed diameter ratio, $D_1/D_{,opt} = 1$, at velocity contours for stenosis degree, S = 75% and Re = 250. (a) α = 30°; (b) α = 40°; (c) α = 50°; (d) α = 60°; (e) α = 70°.

For any degree of stenosis, it is noteworthy that at lower junction angles (Fig. (2.10a), (2.11a) and (2.12a)), smaller peaks of velocity appeared along with the domain, i.e., blood flow was more uniform in both the bypass and the artery. Upstream of the stenosis no significant differences in velocity contours as well as in recirculation zones were noticed. Downstream of the stenosis, at S equal to 50% (Fig. (2.11)) and 75% (Fig. (2.12)), an accentuation of a recirculation zone could be seen near the toe ($\tilde{x}$ = 3 to 5) with the increase of the junction angle. Besides, at S equal to 75% (Fig. (2.12)), the increase of α promoted a greater direction of flow against the bed of the artery ($\tilde{x}$ = 3 to 4). These findings were in line with previous steady and pulsatile studies that stated the anastomotic angles greatly dominate the flow conditions around the heel, toe, and across the artery bed. Lee et al. (2001) and Do et al. (2010) concluded that a smaller angle meant weaker secondary flow and smoother overall flow but in practice it took a longer suture line which would be more vulnerable to thrombosis. Chua et al. (2005a) and Owida et al. (2012) observed that high gradients of velocity were found in the post stenotic region, which might be the reason for the IH to be more prevalent at this region. Regardless of the angle studied in a 70% stenotic artery, Ko et al. (2008) stated that there are four low-velocity regions in the artery and one in the graft. They also concluded that the increase of anastomotic angle caused less percentage of the mass flow rate flowing into the bypass graft but did not influence the flow patterns. Vimmr et al.

(2012) pointed out as a practicable solution an intermediate angle that ensured a relatively uniform flow field but did not require a complicated implementation technique and a longer suture line.

2.3.4 Wall Shear Stress (WSS)

Intimal hyperplasia formation is associated with low WSS values and there is a risk of plaque rupture at high shear stresses (OJHA, 1994; HARUGUCHI et al., 2003; PEIFFER et al., 2013). In this section the focus is on the shear stress behavior at artery wall. Results are shown at *Re* equal to 250, critical stenosis degree equal to 50% and 75% and, similarly to velocity contours, the focus is on the isolated effect on WSS caused by the variation of the diameter ratio D_1/D and junction angle α.

The shear stress found in each point was normalized by the shear stress at a fully developed condition in the host artery. Remarkable results are pointed out at three positions on the wall artery (inner, outer and side wall, as presented in Fig. (2.13) to (2.18)). In any of the three wall positions studied, it was possible to observe that with the increment of the stenosis degree higher WSS values were obtained in the constricted area ($\tilde{x}$ = 0). This result was in agreement with the conclusions of Ko et al. (2007) and Vimmr et al. (2012). Also, by reducing the diameter ratio, there was an expressive increase in WSS values in the area of stenosis ($\tilde{x} = 0$). A less representative increase in WSS occured in same region with increment of junction angle.

At the inner wall (Fig. (2.13) and (2.14)), increasing the diameter ratio or reducing junction angle induced higher WSS values in the entrance of bypass ($\tilde{x}$ = -2 to -1) and toe regions ($\tilde{x}$ = 3 to 4). These results suggested that by increasing the aspect ratio D_1/D and decreasing the angle α, more blood flow was deviated through the bypass.

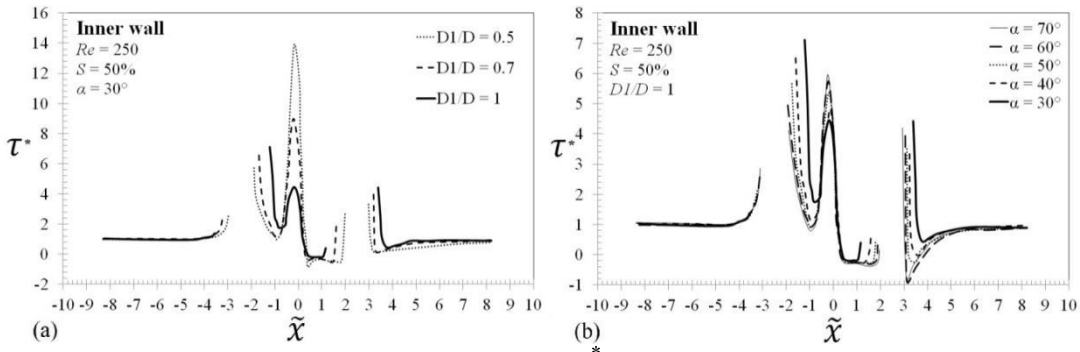

Figure 2.13 – Results of normalized shear stress, τ^*, provided by the variation of (a) diameter ratio, D_1/D and (b) junction angle, α on the inner wall for *S* = 50% and *Re* = 250.

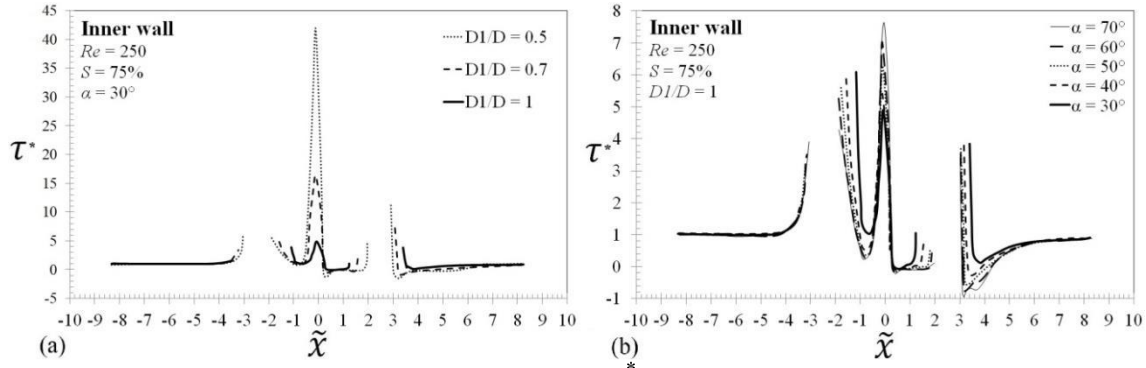

Figure 2.14 – Results of normalized shear stress, τ^*, provided by the variation of (a) diameter ratio, D_1/D and (b) junction angle, α on the inner wall for S = 75% and Re = 250.

Another observation at the inner wall in Fig. (2.13b) and Fig. (2.14b) were the negative values of WSS in the recirculation zones ($\tilde{x}$ = 3 to 4). It was possible to conclude that the increase in junction angle provided a more intense recirculation zone at the toe region ($\tilde{x}$ = 3 to 4). This result was in contrast to Vimmr et al. (2012) which did not observe an appreciable influence of junction angle in the pre and post-stenotic regions. However, in the vicinity of the toe, a larger angle exposed the wall to lower shear stress. Do et al. (2010) also pointed out that by changing the junction angle the WSS locations were more pronounced around the graft and at the bed near the toe.

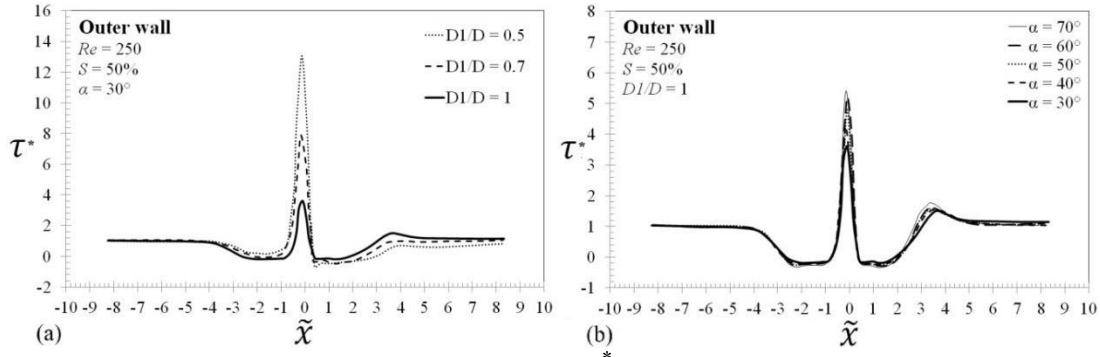

Figure 2.15 – Results of normalized shear stress, τ^*, provided by the variation of (a) diameter ratio, D_1/D and (b) junction angle, α on the outer wall for S = 50% and Re = 250.

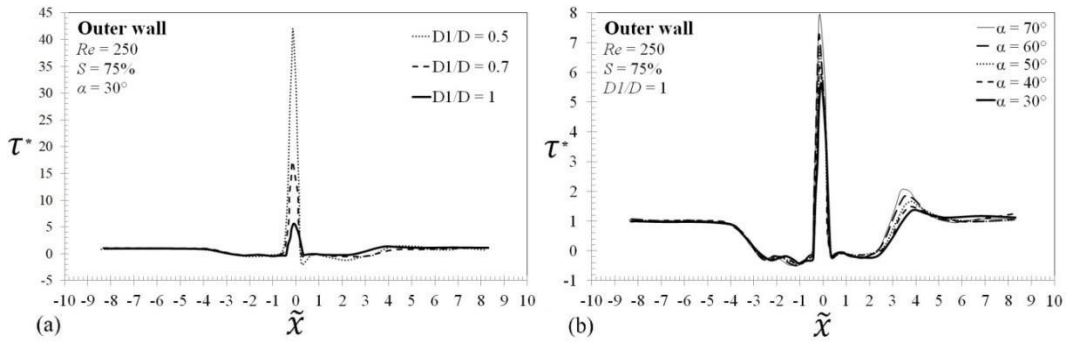

Figure 2.16 – Results of normalized shear stress, τ^*, provided by the variation of (a) diameter ratio, D_1/D and (b) junction angle, α on the outer wall for S = 75% and Re = 250.

On the outer wall (Fig. (2.15) and (2.16)) it is noted the influence on WSS caused by the variation of diameter ratio and junction angle. In Fig. (2.15a), in the post stenotic region ($\tilde{x}$ = 2 to 4) the increase in D_1/D caused higher WSS values. In Fig. (2.16b), the increase in junction angle caused a peak of shear stress in the artery bed ($\tilde{x}$ = 3 to 4). Chua et al. (2005a) and Ko et al. (2008) also reported high gradients of WSS in the post stenotic region at the artery bed by increasing the junction angle, which may be the reason for the thicker intimal hyperplasia at the floor of host artery. All these observations were also noted on the side wall (Fig. (2.17) and (2.18)). The difference is in Fig. (2.17b) and (2.18b) in the region upstream of the stenosis ($\tilde{x}$ = -3 to -2), where greater negative WSS values were observed for larger angles.

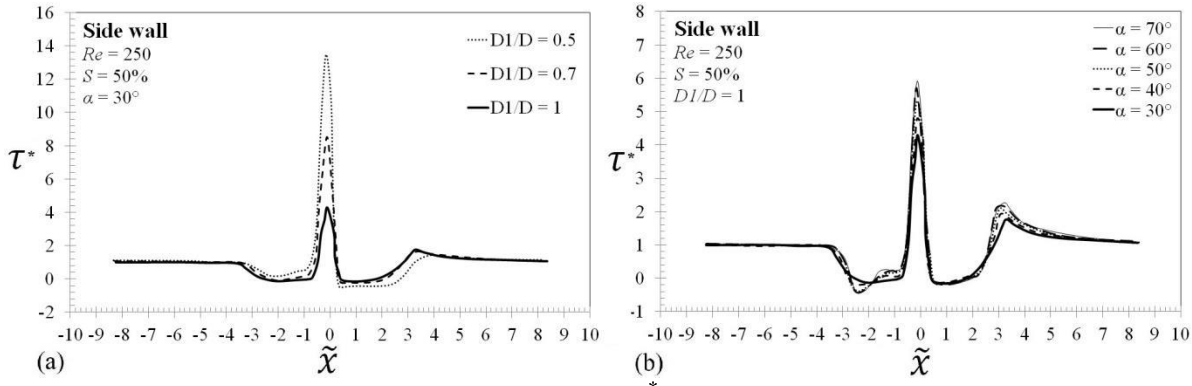

Figure 2.17 – Results of normalized shear stress, τ^*, provided by the variation of (a) diameter ratio, D_1/D and (b) junction angle, α on the side wall for S = 50% and Re = 250.

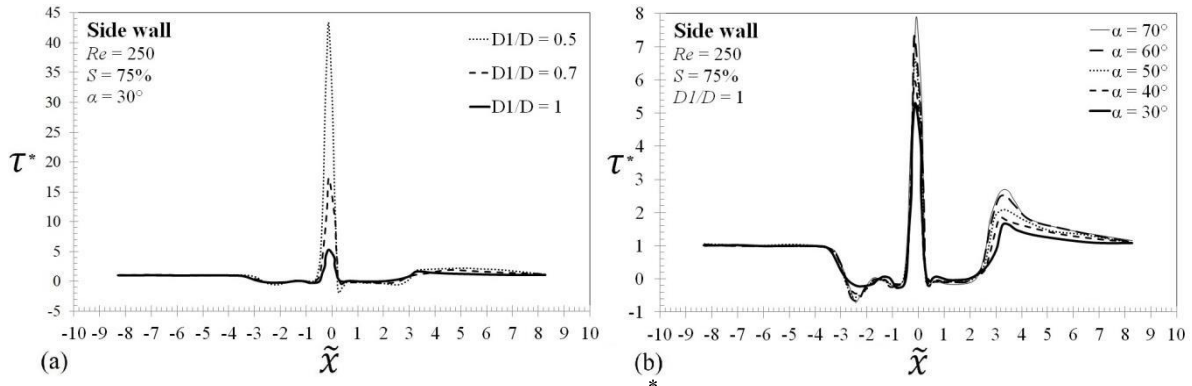

Figure 2.18 – Results of normalized shear stress, τ^*, provided by the variation of (a) diameter ratio, D_1/D and (b) junction angle, α on the side wall for S = 75% and Re = 250.

2.4 CONCLUDING REMARKS

In this work, it was investigated the effects of geometric parameters in different flow conditions of a bypass graft in an idealized, partially-stenosed coronary artery. Using

Constructal Design associated with Design of Experiments and Response Surface methodologies, nine response surfaces were generated, each one representing the results of stenosis degree S equal to 25%, 50%, and 75% and for Reynolds number equal to 150, 250 and 400. It was found for which values of D_1/D and α the dimensionless pressure drop $\tilde{p}$, was minimized. In all situations, as the diameter ratio increased to 1 and the junction angle decreased to 30º, $\tilde{p}$ decreased. Also, it was possible to notice a considerable dependence of $\tilde{p}$ on the stenosis degree S. The optimum point for all cases was $D_1/D_{,opt}$ equal to 1 and $\alpha_{,opt}$ equal to 30°, which was confirmed by previous studies. It was also evaluated the isolated effects on velocity contours and wall shear stress (WSS) caused by the variation of the diameter ratio D_1/D and junction angle α. The results showed that D_1/D had more significant effects than α. It is noteworthy that the Design of Experiments and Response Surface methodologies can be used in the future to evaluate other hemodynamic parameters to improve the results found so far.

At this point, some limitations of this study should be mentioned. First of all, a steady-state condition was applied while the blood flow is known to be pulsating. Secondly, the blood was assumed as a Newtonian fluid, which may affect the results found at low shear stress rates. Moreover, the grafts and arteries were assumed as rigid walls and idealized without considering a patient-specific vascular model. In addition, literature does not yet provide many experimental data that are essential for validation and clinical adoption of any proposed configuration.

Despite the above-mentioned simplifications and assumptions, by applying Constructal Design methodology, the main conclusions and the optimal graft design found in this paper are in accordance with previous studies that evaluated the graft design with other methodologies. It is worth mentioning that until now the few applications of Constructal theory in medicine had been with respect to cancer treatments in two works. One, by Wang et al. (2007) evaluated the crucial problem of keeping the temperature of the healthy tissue surrounding the tumor below a certain threshold so as not to damage the tissue itself. The other, by Lucia and Grisolia (2018) studied the entropy generation related to the pH changes obtained by ionic transport through a membrane related to mitosis/apoptosis ratio and fundamental to evaluate the probability of evolution of cancer. Other two works in the vision area used an approach based on Constructal Law: one to analyse the pressure inside the eye's anterior chamber in relation to the biomechanical properties of corneas (LUCIA et al., 2016) and the other verified how the chloride ions fluxes can determine the water inflow and outflow and to understand how intraocular pressure is controlled by these fluxes (LUCIA et

al., 2017). Finally, starting from the outcomes obtained here, it is evident that the introduction of the Constructal Design method in the area of hemodynamics can provide valuable results for problems that literature still does not provide a definitive clarification.

3 INFLUENCE OF NON-NEWTONIAN BLOOD FLOW ON THE ARTERIAL BYPASS GRAFT CONSTRUCTAL DESIGN

Abstract. *The effect of Newtonian or non-Newtonian model application in hemodynamic characteristics in the cardiovascular system is still debatable, especially on arterial bypass graft designs. In this regard and based on the Constructal Design method, this study seeks to investigate the influence of Carreau rheological parameters, η^*, λ and n, on the flow through a bypass graft circumventing an idealized, partially-stenosed coronary artery. The computational model assumes a steady-state fluid flow through an artery stenosis degree of 75% at two different Reynolds Numbers. A Computational Fluid Dynamics model and a Response Surface Methodology were employed to assess the effects of the project parameters on pressure drop for specific combinations. A comparison between Newtonian and non-Newtonian results was done, through an analysis of the influence of each rheological parameter of the Carreau model for blood. All the response surfaces generated for both the Newtonian and non-Newtonian cases presented a great similarity. It was found for which values of diameter ratio D_1/D and junction angle α the dimensionless pressure drop $\tilde{p}$, was minimized. In all situations, as the diameter ratio increased to 1 and the junction angle decreased to 30º, $\tilde{p}$ decreased. It is possible to notice a considerable dependence of $\tilde{p}$ on the rheological parameters. For the two Reynolds number studied, the Newtonian case presented the lowest value of the dimensionless pressure drop, which can suggest that the choice of applying Newtonian blood may underestimate the value of pressure drop for the system. Even so, the results obtained demonstrate that non-Newtonian rheological parameters did not influence neither the shape of the response surfaces nor the optimum points found, although they have a great impact on pressure drop, mainly η^* and n. Finally, it was also evaluated the effects on velocity and wall shear stress (WSS) caused by the variation of rheological parameters, where, η^* and n, appear to have a more pronounced influence than λ.*

Keywords: *Constructal Design, non-Newtonian blood, Carreau model, coronary artery bypass graft, dimensionless pressure drop.*

3.1 INTRODUCTION

Blood is a suspension of red blood cells (RBC) and plasma with white blood cells and platelets in relatively low volume fractions (HORNER et al., 2018). According to Owens

(2006), blood is essentially a non-Newtonian fluid, showing shear-thinning behaviour, and, additionally, both thixotropic and viscoelastic properties. Johnston et al. (2004) asserted that, despite the considerable amount of viscosity models, none of them fully expresses the effects of the extremely complicated nature of blood rheology. The blood properties are dependent on cell concentration, coagulation, adhesion and oxygen concentration and its viscosity also varies with the hematocrit, which is the percentage of the total blood volume occupied by blood cells (PEREIRA et al., 2013).

In addition, previous studies have shown that the rheological parameters of blood vary from individual to individual and are directly influenced by other several factors, e.g. male or female, smoker or non-smoker, temperature, lipid loading, hypocaloric diet, cholesterol level and physical fitness index (CHO and KENSEY, 1991). Zydney et al. (1991) asserted that red cell deformability causes a decrease in viscosity of blood at high shear rates and red cell aggregation causes a large increase in viscosity at low shear rates for suspensions of red cells. Marcinkowska-Gapinska et al. (2007) studied 100 blood samples of myocardial infarction survivors, treated by different antithrombotic drugs. Their conclusion suggested that acenocoumarol may slightly alter red cell deformability and rouleaux formation, while aspirin does not affect blood rheological properties. Brun et al. (2011) concluded that physiology, not only pathology, is also closely related to hemorheology and may be an important modifier of blood viscosity factors. Guiraudou et al. (2013) demonstrated that the body mass index (BMI) is associated with increase plasma viscosity and red cell rigidity. Brun et al. (2016) confirmed that fat mass is a major regulator of red blood cells aggregation, not only in obese subjects. They also concluded that low hematocrit in athletes may be rather a marker of training volume than fitness. Mehri et al. (2018) performed several experimental tests in a controlled microfluidic system, varying shear rate, three different hematocrits levels, at both room and body temperatures. They studied the effects of temperature, hematocrit, shear rate and viscosity on RBC aggregate sizes. The viscosity data were fitted with two fluid models, power law and Carreau, to obtain the non-Newtonian parameters associated with these models.

Given these circumstances, several authors have studied non-Newtonian blood behavior in the cardiovascular system, especially in stenotic arteries, bifurcations, and ramifications. Cho and Kensey (1991) applied a finite element method to study the effects of the non-Newtonian viscosity of blood on flow through a stenotic coronary arterial bifurcation. They concluded that the non-Newtonian effects must be considered at lower Reynolds numbers, corresponding to a resting state. Gijsen et al. (1999) performed an investigation of the influence of non-Newtonian properties of blood on velocity distribution in a three

dimensional model of the carotid bifurcation. Their conclusion was that the influence of shear thinning properties on velocity distribution is dependent on the alteration of the artery geometry, i.e., in this case bifurcations and diameter variation. An index that quantifies the importance of non-Newtonian effects was defined by Johnston et al. for both steady state (JOHNSTON et al., 2004) and transient state (JOHNSTON et al., 2006). Razavi et al. (2011) applied this index in a numerical study for a carotid artery under symmetrical 30–60% stenosis for Newtonian and six non-Newtonian viscosity models and concluded that the differences between models are more significant at low inlet velocities. Bodnár et al. (2011) compared non-Newtonian fluid models with respect to shear-thinning and viscoelastic effects in the blood flow of stenosed vessels. Their findings suggested that shear-thinning effects are predominant in the recirculation zone downstream the stenosis and they are more pronounced than the viscoelastic ones. Molla and Paul (2012) performed blood flow simulations in a 3D model of a stenotic artery by using five different blood viscosity models. They found that the recirculation zone in the post-stenotic region is enlarged in the non-Newtonian models, which may increase the possibility of blood clot or thrombosis. Tian et al. (2013) simulated a stenosed 2D artery with atherosclerosis and found out that the result of WSS and other shear parameters for a non-Newtonian fluid are smaller than for a Newtonian one. Karimi et al. (2014) studied numerically the flow at a realistic aorta and suggested that various rheological models for blood may be used as alternatives except the Cross model that displays significant discrepancies with all other models at specific points. Fortuny et al. (2015) studied the blood flow in a realistic 3D model of a section of a popliteal vein with a thrombotic mass. Contrasting with previous studies, their findings indicated that non-Newtonian effects are relevant even when higher blood flow rates are considered. Weddell et al. (2015) studied a 3D idealized femoral artery tree and demonstrated differences between Newtonian and Carreau-Yasuda model when velocity, WSS and pressure were compared. They demonstrated that Newtonian velocity profiles are shown to exhibit higher peak magnitudes than the non-Newtonian model within the healthy idealized femoral artery tree. Also, Newtonian pressure is shown to be lower than non-Newtonian. Apostolidis et al. (2016) showed significant differences between the numerical simulations of Newtonian and non-Newtonian models in simplified left coronary artery. Those differences could be noted at the low shear rate regime, where the non-Newtonian effects are primarily manifested. They attributed this phenomenon to the coupling that exists between low and high shear rate areas in the flow, which occur mainly in constrictions and bifurcations. Doost et al. (2016) performed a numerical analysis in human patient-specific left ventricle and suggested that the non-Newtonian models had

significant influence on the intraventricular flow dynamics. They compared the intraventricular flow pattern of different models and observed that the number and magnitude of small vortices for various models were different. They also observed that the WSS maximum value for most non-Newtonian models was significantly higher than the Newtonian model. Iasiello et al. (2017) investigated the non-Newtonian effects on the blood fluid dynamic behavior in an aorta-iliac bifurcation and demonstrated that with reference to the various rheological models, the Newtonian model is found to be more robust at higher velocities than when velocities are lower.

However, fewer works focused their analysis in the non-Newtonian effects at arterial bypass grafts. Abraham et al. (2005) presented a numerical study of non-Newtonian effects on the shape optimization in an idealized 2D arterial graft geometry and concluded that the non-Newtonian effects did not present significant differences in optimal shapes when considering problems involving blood. Chen et al. (2006) applied the Carreau-Yasuda model in a stenosed coronary bypass and concluded that significant differences must be considered in axial velocity profiles, secondary flow streamlines and WSS between the non-Newtonian and Newtonian fluid flows. Results from this study supported that these differences may have significant hemodynamic effects in the host vessel downstream of the graft, where IH predominantly occurs. O´Callaghan et al. (2006) modelled blood using various constitutive equations and demonstrated that the choice of the model has to be based according to the case studied e.g. flow rate, steady or pulsatile flow and geometry. They asserted that a constitutive equation is still not available which adequately describes the viscous properties of blood under all circumstances. For the case studied (a 45º-bypass), the various constitutive models identified areas of relative high/low WSS but their values were quantitatively different. Vimmr and Jonásová (2010) investigated a complete idealized 3D bypass model 100% stenosed using Carreau–Yasuda model and confirmed that the steady non-Newtonian flow showed outstanding differences not only in the values of WSS, but particularly in the velocity distribution and in the shape of the velocity profile. On the other hand, Vimmr et al. (2013) studied single, double and triple aorto-coronary bypasses numerically and demonstrated that non-Newtonian blood flow does not significantly differ from the Newtonian. The most significant changes occurred in areas of little importance to the formation of intimal hyperplasia. They concluded that the diameter of the vessels involved in bypass is more important for the flow and WSS distribution than the application of a non-Newtonian model. Kim et al. (2014) performed a numerical study in an idealized arteriovenous graft and discovered that the variation of hematocrit should be considered in the calculation of

hemodynamic characteristics of this specific graft. They also concluded that the variation of hematocrit should be predicted using a multiphase blood model to avoid the critical range of wall shear stress when hematocrit changes regionally.

Although many works on literature indicate differences between the hemodynamic characteristics on cardiovascular system, Newtonian or non-Newtonian influence on blood flow is still debatable, especially on arterial bypass graft designs. Furthermore, in most previous works that studied non-Newtonian behavior of blood, standard values for rheological parameters were adopted, regardless of the model chosen and not observing the variation that these parameters may suffer due to several factors that were already mentioned.

In this regard, this paper aims to investigate the influence of each rheological parameters of a Carreau fluid model for blood on Constructal Design of an idealized arterial bypass graft subjected to steady blood flow. This study is a companion paper to the previous work (DUTRA et al., 2020) that demonstrated, by applying Constructal Design method, the influence of geometric parameters on the same graft design. The Constructal Law deals with the physical concepts of life, evolution, design, performance and time arrow (BEJAN, 2016). It states that “For a finite-size system to persist in time (to live), it must evolve in such a way that it provides easier access to the imposed currents that flow through it” (BEJAN, 1997). Constructal Design is the study and mathematical modeling of flow systems evolution. It is based on the Constructal Law and is a method to assess the effect of shape and geometry parameters on the performance of systems with the objective of providing easier access to the currents that flow through them (BEJAN and LORENTE, 2008; ROCHA et al., 2017).

3.2 METHODOLOGY

3.2.1 Constructal Design

Fig. (3.1) presents the flow configuration analyzed in this work. It is an idealized version of an artery partially obstructed by fatty material deposition and implanted with a graft with both proximal and distal anastomoses. The artery is represented as the host artery with a diameter equal to D and length equal to L. The main tube undergoes a stenosis that reduces it to diameter D_0. The geometry is symmetric over the center of the stenosis in the axial direction. The graft is placed at a distance L_2 from the center of the stenosis and its diameter is denoted D_1. The junction angle is α and the graft diameter is denoted D_1. L_3 is the distance

from the center where the stenosis begins. The detailed locations of heel, toe, bed, inner-, outer-, and side-walls are indicated in Fig. (3.1).

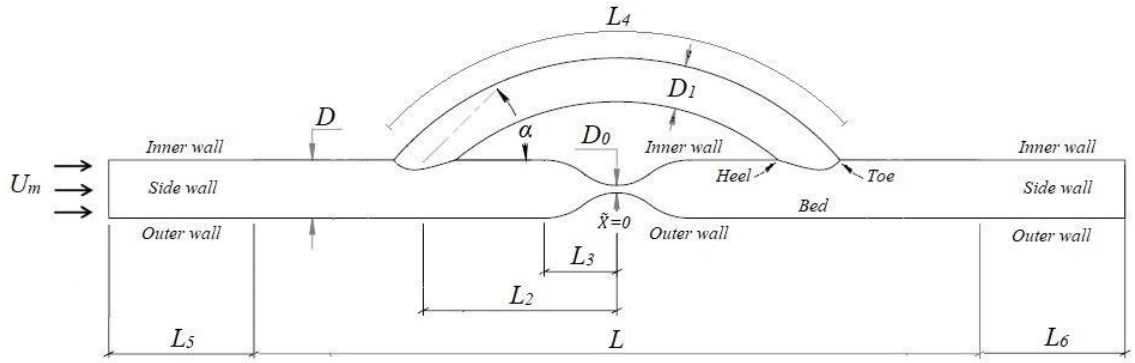

Figure 3.1 – Bypass graft representation.

The flow problem consists of a fluid which enters the domain at the tube inlet with average velocity U_m. Depending on flow conditions and geometry configuration, the flow is partially deviated through the bypass. It is assumed that the tube walls are rigid, impermeable and non-slip. The flow is also assumed to be three-dimensional, steady, incompressible and laminar.

The full computational model for the geometry is depicted in Fig. (3.1) with main tube extensions of 25 diameters upstream and downstream (L_5=*25.D* and L_6=*25.D)* to obtain a fully developed flow. A uniform velocity profile, equal to U_m, was imposed at the inlet. At the outlet, a pressure outlet was imposed as boundary condition. For all simulations, the host artery diameter *D* is equal to 3 mm, corresponding to an average value of the right coronary artery (BERTOLOTTI et al., 2001).

Since the stenosis is usually formed by material deposition, the main tube volume is constant and considered as its external volume was not narrowed:

$$V = \pi \frac{D^2}{4} L \tag{3.1}$$

where *V* is the total artery volume, *D* is the artery diameter and *L* is the total artery length.

The graft volume is

$$V_1 = \pi \frac{{D_1}^2}{4} L_4 \tag{3.2}$$

where V_1 is the total graft volume, D_1 is the graft diameter and L_4 is the total graft length.

The stenosis degree is calculated as

$$S = \frac{D-D_0}{D} x100\% \tag{3.3}$$

where S is the stenosis degree and D_0 is the diameter at the center of the stenosis.

The ratios L/D, L_2/D and L_3/D were defined as constants as detailed in Tab. (3.1). A baseline case from literature (VIMMR et al., 2012) was used in the definition of these values.

Table 3.1 – Geometric parameters for artery and graft build up.

Parameters	Values
L/D	16.67
L_2/D	2.5
L_3/D	1

A critical stenosis degree S equal to 75% was evaluated at two different Reynolds Number, (150 and 250). Blood is modelled as an incompressible Newtonian fluid and non-Newtonian fluid with a shear-thinning fluid behavior, using the Carreau model (CARREAU, 1972).

Constructal Theory assumes that living systems evolve limited by space (ROCHA et al., 2017). Accordingly, Constructal Theory systems must evolve in order to provide easier access to its flows (BEJAN and LORENTE, 2008). To this end, it was considered that the dimensionless pressure drop $\tilde{p}$ along the length L should be as low as possible.

Thus, an optimization problem was formulated as: "Find the minimum $\tilde{p}$. The design variables are the diameter ratio D_1/D and the junction angle α. The restrictions are constant L/D, L_2/D and L_3/D." Therefore, the degrees of freedom for this problem are the diameter ratio D_1/D and the junction angle α. A search is conducted for the diameter ratio D_1/D and junction angle α that minimize the value of the pressure drop $\tilde{p}_{min}$ for specific combinations of Carreau rheological parameters and Reynolds Number Re. A comparison between the Newtonian and non-Newtonian results was done, being analyzed the influence of each rheological parameters of the Carreau model for blood. Figure (3.2) details all the steps required by the Constructal Design methodology.

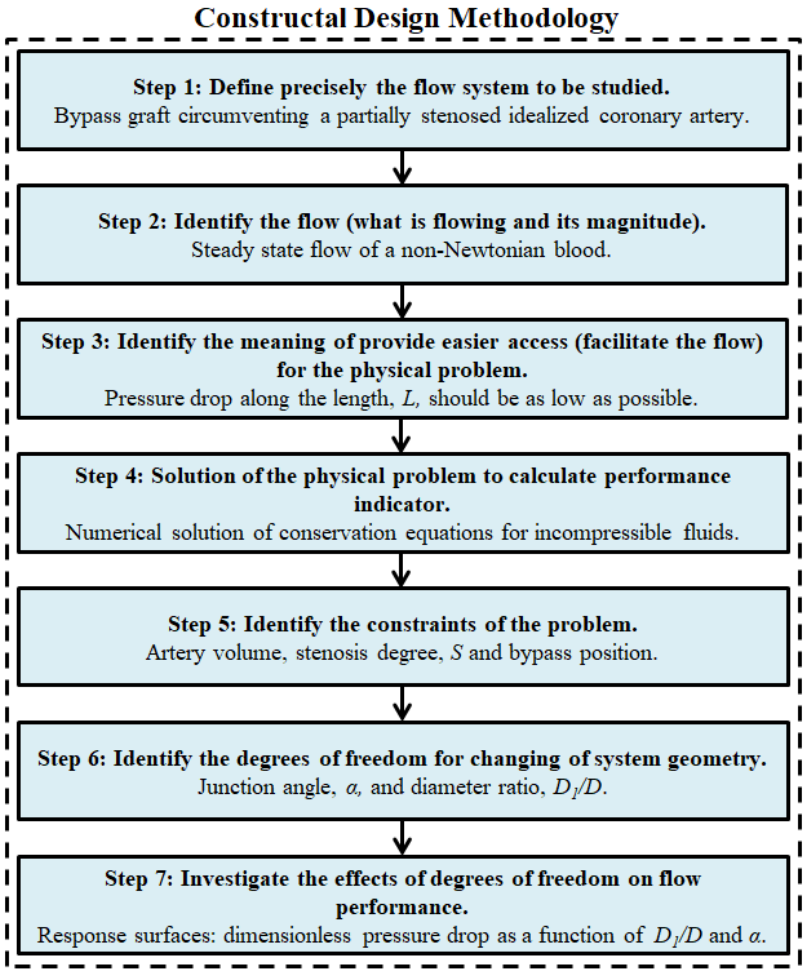

Figure 3.2 – Flowchart with application of Constructal Design and response surfaces for the case studied.

3.2.2 Mathematical Modeling

The mathematical modeling for the flow through the artery and bypass model consists of the mass and momentum balance equations for incompressible fluids. It is written these equations in their dimensionless form as follows:

$$\frac{\partial \tilde{u}_i}{\partial \tilde{x}_i} = 0 \tag{3.4}$$

$$\tilde{u}_i \frac{\partial \tilde{u}_i}{\partial \tilde{x}_j} = -\frac{\partial \tilde{p}}{\partial \tilde{x}_i} + \frac{1}{Re}\frac{\partial \tilde{\tau}_{ij}}{\partial x_j} \tag{3.5}$$

where $\tilde{u}_i$ denotes the dimensionless velocity field, $\tilde{x}_i$ the dimensionless position vector, $\tilde{p}$ the dimensionless pressure drop, $\tilde{\tau}_{ij}$ the dimensionless extra stress tensor field, Re the Reynolds number such that:

$$\tilde{u}_i = \frac{u_i}{U_m}; \qquad \tilde{x}_i = \frac{x}{D}; \qquad \tilde{p} = \frac{\Delta p}{\rho {U_m}^2}; \qquad \tilde{\tau} = \frac{\tau_{ij}}{(U_m \eta_c)/D} \qquad Re = \frac{\rho U_m D}{\eta_c} \tag{3.6}$$

where Δp is the pressure drop along L, ρ is the fluid mass density, U_m is the average velocity at the inlet and η_c is the characteristic viscosity.

The constitutive equation for the extra stress is that of a generalized Newtonian liquid:

$$\tau_{ij} = 2\eta(\dot{\gamma}) D_{ij} \tag{3.7}$$

where $\eta(\dot{\gamma})$ is the viscosity function and D_{ij} is the strain rate tensor, given as the symmetric part of the velocity gradient tensor (SLATTERY, 1999). The Carreau equation was employed to model the behavior of shear-thinning fluids (CARREAU, 1972):

$$\eta(\dot{\gamma}) = \eta_\infty + (\eta_0 - \eta_\infty)(1 + (\lambda\dot{\gamma})^2)^{\frac{n-1}{2}} \tag{3.8}$$

where η_0 is the zero shear rate viscosity, η_∞ is the infinite shear rate viscosity, λ is a time constant, n is the power-law index. The dimensionless form of this model is:

$$\tilde{\eta} = 1 + (\eta^* - 1)(1 + (\dot{\gamma}^*)^2)^{\frac{n-1}{2}} \tag{3.9}$$

where

$$\tilde{\eta} = \frac{\eta(\dot{\gamma})}{\eta_\infty}; \qquad \eta^* = \frac{\eta_0}{\eta_\infty}; \qquad \dot{\gamma}^* = \frac{\dot{\gamma}}{\lambda} \tag{3.10}$$

For shear-thinning fluid flows, one dimensionless group for dynamic similarity is the Carreau number (DE SOUZA MENDES, 2007):

$$\tilde{\lambda} = \frac{\lambda U_m}{D} \tag{3.11}$$

3.2.3 Rheological parameters

An extensive literature research was conducted to evaluate which rheological parameters were applied in the previous studies that used Carreau fluid model for blood. Table (3.2) summarizes the main cases and the respective values adopted.

Table 3.2 – Literature research of Carreau parameters for blood.

Authors	η^*	λ	n	Hematocrit	Temperature
Cho and Kensey (1991)	16.2	3.313	0.3568	40%	-
Johnston et al. (2004)	16.2	3.313	0.3568	-	-
Molla and Paul (2012)	16.2	3.313	0.3568	-	-
Pereira et al. (2013)	14.3	3.313	0.3440	-	-
Pereira et al. (2013)	16.2	3.313	0.3568	-	-
Pereira et al. (2013)	7.1	25	0.2500	-	-
Karimi et al. (2014)	16.0	3.313	0.3568	40%	-
Fortuny et al. (2015)	16.2	3.313	0.3568	-	-
Doost et al. (2016)	16.0	3.313	0.3568	-	-
Iasiello et al. (2017)	16.2	3.313	0.3568	-	-
Mehri et al. (2018)	16.8	3.313	0.3530	5%	23°C
Mehri et al. (2018)	56.2	3.312	0.3690	10%	23°C
Mehri et al. (2018)	11.5	3.313	0.3520	5%	37°C
Mehri et al. (2018)	51.6	3.312	0.3620	15%	23°C
Mehri et al. (2018)	10.2	3.312	0.3530	10%	37°C
Mehri et al. (2018)	16.2	3.313	0.3560	45%	37°C
Mehri et al. (2018)	33.2	3.314	0.1520	15%	37°C

It is important to note that few studies in Tab. (3.2) reported the percentage of hematocrit considered and only the experimental work by Mehri et al. (2018) collected the influence of hematocrit and temperature on blood parameters. In this sense, the present work selects and simulates extrapolated ranges of rheological parameters of Carreau, as presented in Tab. (3.3), to verify the influence of each one in the Constructal Design.

Table 3.3 – Range of rheological parameters of the Carreau blood model.

Parameters	Values
η^*	15 – 1000
λ	3 – 50
n	0.35 – 0.60

3.2.4 Numerical Method and Computational Grid

In order to solve the system of partial differential equations, the Finite Volume Method (PATANKAR, 1980) was employed using the ANSYS/FLUENT v. 18.2 (ANSYS, 2015). A pressure-based solver was used with a pressure-velocity coupling method and second-order interpolation functions for pressure and velocity fields. All calculations were conducted in double-precision representation of real numbers. The iterative algorithm was a false transient. The mesh was parameterized to keep proportional the element sizes according to the diameter ratio studied. Depending on the configuration, a total of 500,000 to 950,000 tetrahedral finite elements were necessary to mesh the computational domain accurately. Along the walls, prismatic layers elements were used in order to better capture the boundary layer. Figure (3.3) presents a sample of the computational mesh for the model with detailed views at the cross section in the bypass and native stenotic artery. As convergence criterion, scaled residuals of each equation at an iteration were used and compared with a user-defined convergence criteria equal to 10^{-6} for velocity and pressure fields.

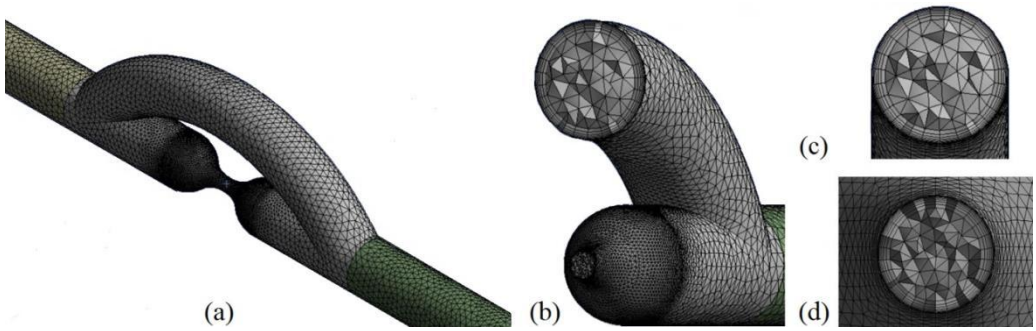

Figure 3.3 – Isometric view of the computational mesh for the model (a) with a detailed view at the cross section in the bypass and native stenotic artery (b) and a front mesh view of the bypass (c) and stenosis region (d).

For the previous Newtonian case (DUTRA et al., 2020), the *Grid Convergence Index (GCI)* method was applied for different values of junction angle α and diameter ratio D_1/D in three different values of stenosis degree (S = 25%, 50%, and 75%). As explained by Celik et al. (2008), this method is useful for calculation and reporting of discretization error estimates in CFD simulations where experimental data may not be available for comparison. Table (3.4) presents a comparing between the two higher *GCI* found for Newtonian blood and the respective *GCI* values for non-Newtonian blood in the same bypass configuration. The number of elements is represented by *N*. Thus, it can be verified that the maximum *GCI* for

the non-Newtonian case was 1.14%, refining the mesh in the same factor of 15% to 30%. It is important to observe that, based on experience and not on formal derivation, a maximum GCI value of 5% is considered acceptable for this method (CELIK et al., 2008).

Table 3.4 – *Grid Convergence Index (GCI)* comparison between the Newtonian and non-Newtonian cases for the same bypass configurations at *Re = 250*.

	Newtonian Case 1	non-Newtonian Case 1	Newtonian Case 2	non-Newtonian Case 2
D_1/D	1	1	1	1
α	70°	70°	70°	70°
S	25%	25%	75%	75%
μ	0.0035	-	0.0035	-
η^*	-	15	-	15
λ	-	3	-	3
n	-	0.35	-	0.35
N1	510,872	510,872	803,049	803,049
N2	434,428	434,428	651,633	651,633
N3	368,760	368,760	490,328	490,328
$\tilde{p}_{,N1}$	2.362	2.641	3.924	4.107
$\tilde{p}_{,N2}$	2.415	2.601	3.928	4.097
$\tilde{p}_{,N3}$	2.437	2.598	3.929	4.036
GCI	**1.82%**	**1.14%**	**1.66%**	**1.12%**

3.2.5 Design of Experiments and Response Surface Methodology

To investigate the effects of the junction angle α and the artery diameter ratio D_1/D on the pressure drop along the length L, the Response Surface methodology available in ANSYS Design Xplorer 18.2 was applied (ANSYS, 2016). A sparse grid method (MONTGOMERY, 2013) was employed for the design of experiments to build the response surfaces and represent $\tilde{p}$ as a function of the degrees of freedom D_1/D and α, within the ranges $0.1 \leq D_1/D \leq 1.0$ and $30^o \leq \alpha \leq 70^o$. Sparse Grid is an adaptive model driven by the accuracy defined by the user. Initially, the program calculated four design points located at the edges and one design point located at the center of the response surface. Then, the response surface was elaborated with a maximum number of 1,000 design points per surface. This method increases the accuracy of the response surface by automatically refining the matrix of design points in locations where the relative error of the output parameter is higher, i.e., it refines design points only in the directions necessary (ANSYS, 2016). It is noteworthy that each design

point represents a specific bypass configuration within the ranges $0.1 \leq D_1/D \leq 1.0$ and $30^o \leq \alpha \leq 70^o$. In this study, the number of points needed to construct each surface ranged from 200 to 300.

After building the response surfaces, the method suggests verification points. It was performed ten verification points (individual simulations) for each response surface. Here the root mean square error (RMSE) was employed as an indicator of the quality of the response surface. The RMSE is defined as

$$RMSE = \sqrt{\frac{1}{m}\sum_{i=1}^{m}\left(\frac{\tilde{p}_{pred,i} - \tilde{p}_{obs,i}}{\tilde{p}_{obs,i}}\right)^2} x100 \tag{3.12}$$

where $\tilde{p}_{pred}$ is the value of $\tilde{p}$ predicted from response surface, $\tilde{p}_{obs}$ is the value of $\tilde{p}$ observed from the verification points, and m is the number of verification points.

In all cases, there was a good agreement between individual simulations and the response surfaces. The maximum RMSE for the response surfaces presented in this work was of 1.21%.

3.3 RESULTS AND DISCUSSION

3.3.1 Response Surfaces

Eighteen response surfaces were generated applying the sparse grid method (MONTGOMERY, 2013). Figure (3.4) presents a comparison between two samples of response surfaces that represent $\tilde{p}$ as a function of the degrees of freedom, D_1/D and α, within the ranges $0.1 \leq D_1/D \leq 1.0$ and $30^o \leq \alpha \leq 70^o$. Figure (3.4a) represents the Newtonian case (μ = 0.0035 Pa.s / η^* = 1) while Fig. (3.4b) exhibits the non-Newtonian baseline case (η^* = 15; λ = 3; n = 0.35). Both response surfaces represent the results of stenosis degree S equal to 75% at Reynolds Number Re equal to 150.

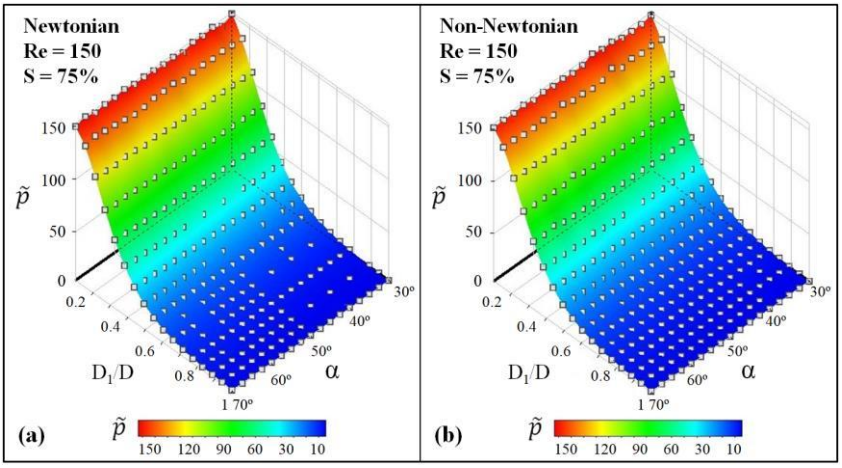

Figure 3.4 – Response surfaces representing $\tilde{p}$ as a function of D_1/D and α for the stenosis degree equal to 75% and Reynolds number equal to 150: (a) Newtonian case (μ = 0.0035 Pa.s); (b) non-Newtonian baseline case (η^* = 15; λ = 3; n = 0.35).

A great similarity could be seen in all the response surfaces generated for both the Newtonian and non-Newtonian cases. It is possible to observe that both response surfaces had a specific optimal point that minimized the dimensionless pressure drop $\tilde{p}$. For each case, a value of D_1/D and α where $\tilde{p}$ is minimum was obtained. In all situations, as the aspect ratio D_1/D increased to 1 and the junction angle, α, decreased to 30º, $\tilde{p}$ decreased. As the flow is highly deviated through the bypass, the influence of α in $\tilde{p}$ became almost unnoticeable.

Table (3.5) and (3.6) summarize the optimal geometry results for the eighteen configurations. The parameter λ is represented in the table by the Carreau Number, $\tilde{\lambda}$, which accounts for the effects of varying λ in the viscosity function (ZINANI and FREY, 2008). It is possible to notice a considerable dependence of $\tilde{p}$ on the rheological parameters, especially η^* and n. Also, the optimum point for all cases was $D_1/D_{,opt}$ equal to 1 and $\alpha_{,opt}$ equal to 30°.

Table 3.5 – Optimum results for stenosis degree equal to 75%, at *Re* equal to 150.

Re	*Case*	μ	η^*	λ	$\tilde{\lambda}$	n	$\tilde{p}_{,min}$	$D_1/D_{,opt}$	$\alpha_{,opt}$
	Newtonian	0.0035	1	-	-	-	3.978	1	30°
	Non-Newtonian	-	15	3	175	0.35	4.472	1	30°
	Non-Newtonian	-	15	3	175	0.60	6.750	1	30°
	Non-Newtonian	-	15	50	2916.7	0.35	4.054	1	30°
150	Non-Newtonian	-	15	50	2916.7	0.60	4.853	1	30°
	Non-Newtonian	-	1000	3	175	0.35	38.237	1	30°
	Non-Newtonian	-	1000	3	175	0.60	207.53	1	30°
	Non-Newtonian	-	1000	50	2916.7	0.35	9.517	1	30°
	Non-Newtonian	-	1000	50	2916.7	0.60	69.217	1	30°

Table 3.6 – Optimum results for stenosis degree equal to 75%, at *Re* equal to 250.

Re	*Case*	μ	η^*	λ	$\tilde{\lambda}$	n	$\tilde{p}_{,\min}$	$D_1/D_{,\text{opt}}$	$\alpha_{,\text{opt}}$
	Newtonian	0.0035	1	-	-	-	2.659	1	30°
	Non-Newtonian	-	15	3	291.7	0.35	2.866	1	30°
	Non-Newtonian	-	15	3	291.7	0.60	3.992	1	30°
	Non-Newtonian	-	15	50	4861.1	0.35	2.710	1	30°
250	Non-Newtonian	-	15	50	4861.1	0.60	3.091	1	30°
	Non-Newtonian	-	1000	3	291.7	0.35	17.621	1	30°
	Non-Newtonian	-	1000	3	291.7	0.60	103.93	1	30°
	Non-Newtonian	-	1000	50	4861.1	0.35	5.238	1	30°
	Non-Newtonian	-	1000	50	4861.1	0.60	35.444	1	30°

For the two Reynolds number studied, the Newtonian case presented the lowest value of the dimensionless pressure drop. This finding suggests that the choice of applying Newtonian blood may underestimate the value of pressure drop for the system. Weddell et al. (2015) reached the same result in their study of an artery tree, where the Newtonian pressure drop found was lower than non-Newtonian one.

Even so, the results obtained demonstrate that non-Newtonian rheological parameters did not influence neither the shape of the response surfaces nor the optimum points found. On the previous paper (DUTRA et al., 2020), that applied the Newtonian model, the same optimum point was found for different stenosis degree *S* equal to 25%, 50% and 75% at three different Reynolds Number. Likewise, these discoveries are in line with the work of Abraham et al. (2005) who verified no significant differences on the optimal junction angle obtained using both the Newtonian and generalized Newtonian constitutive equation. More recently, Vimmr et al. (2013) suggested that the diameter of the vessels involved in the bypassing is a more important parameter than the application of a non-Newtonian model. They asserted that, both for the Newtonian and non-Newtonian case, the bypass diameter is the main determinant parameter for the patency and overall performance of the implanted bypass grafts.

3.3.2 Velocity fields and stream lines

Velocity field data is presented in Fig. (3.5) for the optimum junction angle, $\alpha_{,opt}$ = 30° and diameter ratio, $D_1/D_{,opt}$ = 1 (as found in Tab. (3.5)), at *Re* equal to 150 and for *S* equal to 75%. The Newtonian case and four specific non-Newtonian cases were compared and the main focus was on the effect provided by the variation of rheological parameters.

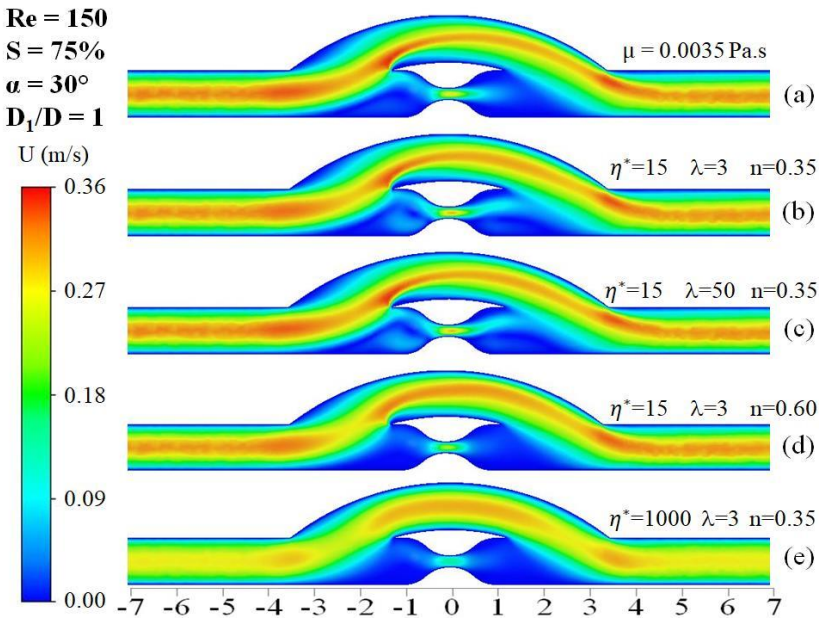

Figure 3.5 – Effect provided by the variation of rheological parameters in the optimum junction angle, $\alpha_{,opt}$ = 30° and diameter ratio, $D_1/D_{,opt}$ = 1, at velocity contours for stenosis degree, S = 75% and Re = 150. Newtonian case (a) μ = 0.0035 Pa.s; and non-Newtonian cases (b) η^*=15; λ=3; n=0.35; (c) η^*=15; λ=50; n=0.35; (d) η^*=15; λ=3; n=0.60; (e) η^*=1000; λ=3; n=0.35.

In general, the first three bypasses, Fig. (3.5a-c), present a similar velocity field, while the last two, Fig. (3.5d-e), differ from the others. This can be explained by the variation of blood rheological parameters, η^* and n, which appear have a more pronounced influence on velocity field than λ. For higher η^* values (Fig. (3.5e)), the most significant change in flow can be noted. This is explained by the greater drop in viscosity curve that occurred in this case between η_0 plateau and the η_∞ plateau. For lower η^* values (Fig. (3.5a-d)), the drop in viscosity does not cause noticeable changes in flow.

Besides, it is possible to assert that, by decreasing the bypass diameter, the non-Newtonian effects on the flow would be more relevant, because the shear rate would increase with the diameter´s reduction, causing a drop in blood viscosity. Nonetheless, as demonstrated in the previous paper (DUTRA et al., 2020), smaller diameters cause a greater pressure drop, which is not desired for the bypass performance.

In addition, with the variation of blood parameters, it is possible to note different flow zones in the region upstream of stenosis ($\tilde{x}$ = -2 to 0). Another changes occurred at the stenosis region ($\tilde{x}$ = 0) where the shear-thinning characteristics of blood affect the jet flow. It is noteworthy that this phenomenon occurs due to the increase in the shear rate caused by the sudden reduction in the diameter of the artery (stenosis). The complexity of these flow

patterns on non-Newtonian blood had been analyzed by Sood et al. (2018) who investigated the flow of Newtonian and non-Newtonian fluid through axisymmetric and asymmetric stenotic artery models and observed that flow patterns are extremely complex in the post stenotic region for both models. However, its role as a pathological determinant was still less understood (ANDERSSON et al., 2019).

Stream lines were generated to understand the differences in the regions upstream ($\tilde{x}$ = -2 to 0) and downstream ($\tilde{x}$ = 0 to 2) of stenosis occurred in Fig. (3.5). Figure (3.6) presents this stream lines at the same flow configurations.

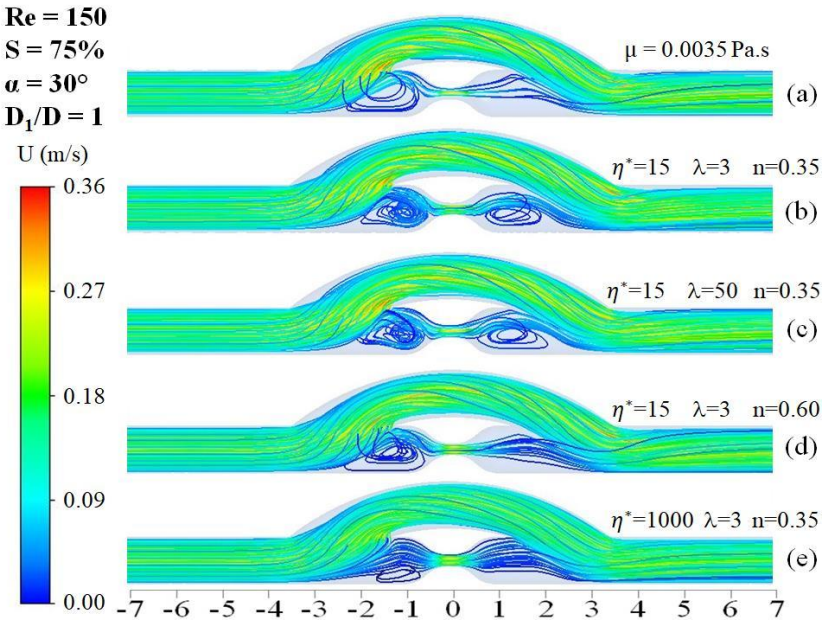

Figure 3.6 – Effect provided by the variation of rheological parameters in the optimum junction angle, $\alpha_{,opt}$ = 30° and diameter ratio, $D_1/D_{,opt}$ = 1, at stream lines for stenosis degree, S = 75% and Re = 150. Newtonian case (a) μ = 0.0035 Pa.s; and non-Newtonian cases (b) η^*=15; λ=3; n=0.35; (c) η^*=15; λ=50; n=0.35; (d) η^*=15; λ=3; n=0.60; (e) η^*=1000; λ=3; n=0.35.

It is noteworthy that larger recirculation zones appeared in the all bypasses, Fig. (3.6a-e), in the region upstream of stenosis while downstream of stenosis only Fig. (3.6b-c) presented this phenomenon. As previously presented, the last two, Fig. (3.5d-e), differ from the others due to the variation of the rheological parameters and the shear-thinning effects. Vimmr and Jonášová (2010) also observed differences in the velocity distribution and in the shape of the velocity profile.

The appearance of recirculation zones should be mentioned, especially downstream of stenosis, where the occurrence of Intimal Hyperplasia is known to be more prevalent. So, this finding demonstrates the importance of choosing a non-Newtonian model for blood because

the choice of a Newtonian model may underestimate this phenomenon. This situation was already well reported by several authors. Chen et al. (2006) concluded that a simple Newtonian fluid model for the blood may lead to false interpretation of experimental observations, particularly when complex vascular geometries are considered. O´Callaghan et al. (2006) stated that when modelling blood computationally, blood cannot be treated as a Newtonian/non-Newtonian fluid in general and under all circumstances. They asserted that is more meaningful to consider each case individually depending on which configuration is under investigation. Vimmr and Jonášová (2010) studied a femoral bypass model and observed several suppressed recirculation zones such as the one usually located before the occlusion. They also suggested that the blood non-Newtonian behaviour was particularly evident in the region downstream from the stenosis.

3.3.3 Wall Shear Stress (WSS)

In this section the focus is on the shear stress behavior at artery wall caused by the variation of rheological parameters of blood. Results are shown at *Re* equal to 150 and stenosis degree *S* equal to 75%. The shear stress found in each point was normalized by the shear stress at a fully developed condition in the host artery. Remarkable results are pointed out at three positions on the wall artery (inner, outer and side wall, as presented in Fig. (3.7) to (3.9)).

In any of the three wall positions studied, it was possible to observe that higher normalized WSS values were obtained in the constricted area ($\tilde{x}$ = 0) for the Newtonian case (μ = 0.0035 Pa.s) and the non-Newtonian baseline case (η^* = 15; λ = 3; n = 0.35). A less representative increase in normalized WSS occurred in same region for other non-Newtonian configurations.

At the inner wall, Fig. (3.7), the Newtonian case (μ = 0.0035 Pa.s) and the non-Newtonian baseline case (η^* = 15; λ = 3; n = 0.35) induced higher normalized WSS values in the entrance of bypass ($\tilde{x}$ = -2 to -1) and toe regions ($\tilde{x}$ = 3 to 4). Also, as shown in the previous section, it is important to point out the presence of negative values of WSS in the recirculation zones near stenosis ($\tilde{x}$ = -1 to 0) and ($\tilde{x}$ = 0 to 1). Chen et al. (2006) also observed flow recirculation downstream of the stenosis near the top wall and rapid changes in WSS in all cases near the heel of bypass.

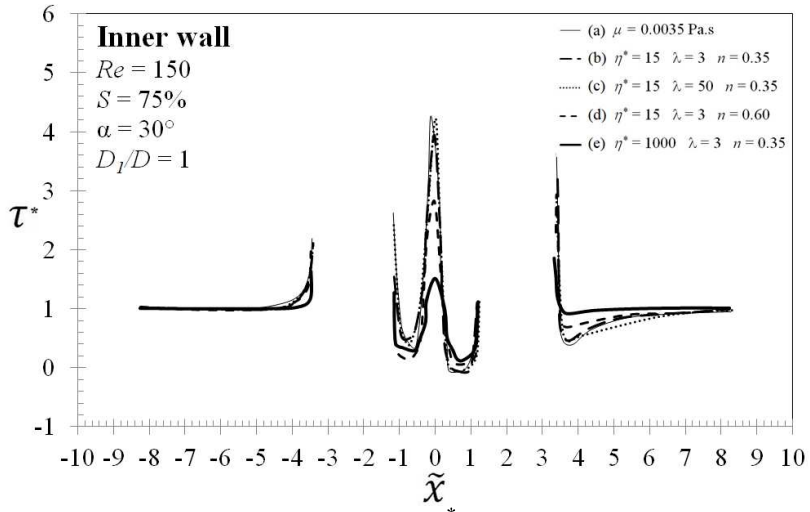

Figure 3.7 – Results of normalized shear stress, τ^*, on inner wall provided by the variation of rheological parameters in the optimum junction angle, $\alpha_{,opt}$ = 30° and diameter ratio, $D_1/D_{,opt}$ = 1, for stenosis degree, S = 75% and Re = 150. Newtonian case (a) μ = 0.0035 Pa.s; and non-Newtonian cases (b) η^*=15; λ=3; n=0.35; (c) η^*=15; λ=50; n=0.35; (d) η^*=15; λ=3; n=0.60; (e) η^*=1000; λ=3; n=0.35.

On the outer wall (Fig. (3.8)) and side wall (Fig. (3.9)) it is noted a great similarity between the results. For both, the most remarkable occurrence is the presence of negative values of WSS in the recirculation zones near stenosis ($\tilde{x}$ = -1 to 0) and ($\tilde{x}$ = 0 to 1) and a peak of shear stress in the artery bed ($\tilde{x}$ = 3 to 4). It is important to observe that the Newtonian and most non-Newtonian results have a similar behavior, with the exception of the non-Newtonian case with higher η^* value (Fig. (3.8e) and (3.9e)), which is also explained by the greater drop in viscosity curve that occurred in this case between η_0 plateau and the η_∞ plateau. Vimmr et al. (2013) asserted that the most significant changes in WSS have local character and are observed mainly upstream from the stenosis, i.e., in areas of little importance to the formation of intimal hyperplasia.

Finally, it is noteworthy that the WSS values shown in Fig. (3.7) to (3.9) have been normalized by the shear stress at a fully developed condition in the host artery. This means that the nominal WSS values for each case are quantitatively very different, especially for higher η^* values. In this point of view, O´Callaghan et al. (2006) stated that the results between Newtonian and non-Newtonian blood are qualitatively but not quantitatively similar. This situation should be considered when comparing different researchers work.

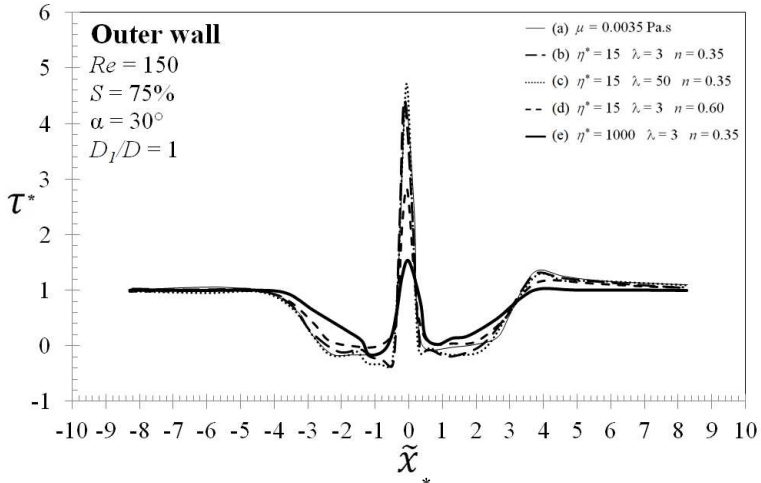

Figure 3.8 – Results of normalized shear stress, τ^*, on outer wall provided by the variation of rheological parameters in the optimum junction angle, $\alpha_{,opt}$ = 30° and diameter ratio, $D_1/D_{,opt}$ = 1, for stenosis degree, S = 75% and Re = 150. Newtonian case (a) μ = 0.0035 Pa.s; and non-Newtonian cases (b) η^*=15; λ=3; n=0.35; (c) η^*=15; λ=50; n=0.35; (d) η^*=15; λ=3; n=0.60; (e) η^*=1000; λ=3; n=0.35.

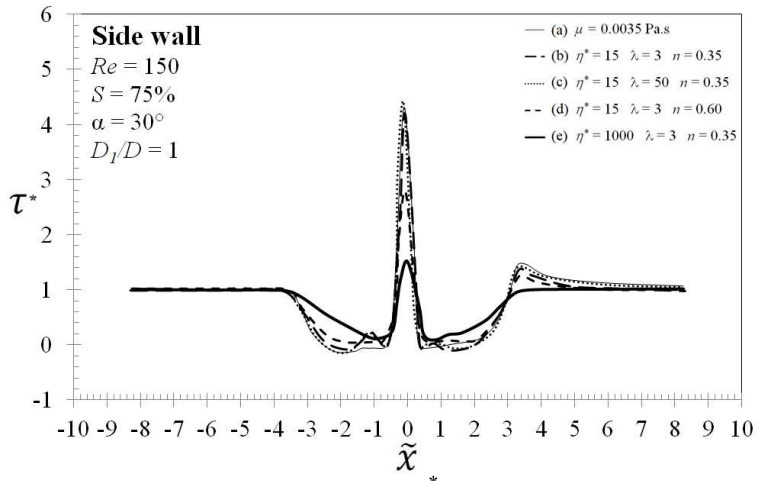

Figure 3.9 – Results of normalized shear stress, τ^*, on side wall provided by the variation of rheological parameters in the optimum junction angle, $\alpha_{,opt}$ = 30° and diameter ratio, $D_1/D_{,opt}$ = 1, for stenosis degree, S = 75% and Re = 150. Newtonian case (a) μ = 0.0035 Pa.s; and non-Newtonian cases (b) η^*=15; λ=3; n=0.35; (c) η^*=15; λ=50; n=0.35; (d) η^*=15; λ=3; n=0.60; (e) η^*=1000; λ=3; n=0.35.

3.4 CONCLUDING REMARKS

In this work, it was investigated the effects of rheological parameters in different flow conditions of a bypass graft in an idealized, partially-stenosed coronary artery. Using Constructal Design associated with Design of Experiments and Response Surface methodologies, eighteen response surfaces were generated applying the sparse grid method, each one representing the results of stenosis degree S equal to 75% for specific combinations

of Carreau rheological parameters and Reynolds Number *Re* equal to 150 and 250. A comparison between the Newtonian and non-Newtonian results was done, being analyzed the influence of each rheological parameters of the Carreau model for blood.

All the response surfaces generated for both the Newtonian and non-Newtonian cases presented a great similarity. It was found for which values of D_1/D and α the dimensionless pressure drop $\tilde{p}$, was minimized. In all situations, as the diameter ratio increased to 1 and the junction angle decreased to 30º, $\tilde{p}$ decreased. It is possible to notice a considerable dependence of $\tilde{p}$ on the rheological parameters. Also, the optimum point for all cases was $D_1/D_{,opt}$ equal to 1 and $\alpha_{,opt}$ equal to 30°. On the previous paper (DUTRA et al., 2020), that applied the Newtonian model, the same optimum point was found for three different stenosis degree *S* equal to 25%, 50% and 75% at three different Reynolds Number (150, 250 and 400).

For the two Reynolds number here studied, the Newtonian case presented the lowest value of the dimensionless pressure drop, which can suggest that the choice of applying Newtonian blood may underestimate the value of pressure drop for the system. Even so, the results obtained demonstrate that non-Newtonian rheological parameters did not influence neither the shape of the response surfaces nor the optimum points found. Besides, it was also evaluated the effects on velocity and wall shear stress (WSS) caused by the variation of rheological parameters, where, η^* and n, appear to have a more pronounced influence on velocity than λ. The rheological parameters also affected the appearance of recirculation zones, especially downstream of stenosis, where the occurrence of Intimal Hyperplasia is known to be more prevalent. On WSS, it is important to observe that the Newtonian and most non-Newtonian results have a similar behavior, with the exception of the non-Newtonian case with higher η^* value, which is explained by the greater drop in viscosity curve that occurred in this case.

At this point, some limitations of this study should be mentioned. First of all, a steady-state condition was applied while the blood flow is known to be pulsating. Moreover, the grafts and arteries were assumed as rigid walls and idealized without considering a patient-specific vascular model. In addition, literature does not yet provide many experimental data that are essential for validation and clinical adoption of any proposed configuration.

Despite the above-mentioned simplifications and assumptions, by applying Constructal Design methodology, the main conclusions and the optimal graft design found in this paper are in accordance with previous Newtonian and non-Newtonian studies that evaluated the graft design with the same and other methodologies.

4 CONCLUSION

Constructal Design is the study and mathematical modeling of flow systems evolution. It has the capability to explain the configuration of existing systems in nature and serve as a conceptual basis for directing engineering projects that aim at improving or optimizing performance. Until now the few applications of Constructal Theory in medicine were within the field of cancer treatments and vision area. So, this work studied numerically the blood flow in a bypass graft implanted in a partially stenosed coronary artery, by applying the Constructal Design to investigate the configurations with best performances and understand the role of fluid rheology on design performance. The results of this dissertation were presented in the form of two articles that composed chapters 2 and 3. In this last chapter, the main findings in these articles were summarized.

Chapter 2 introduced Constructal Design in the hemodynamics area and investigated numerically the effect of geometric parameters on the flow through a bypass graft circumventing a partially stenosed idealized coronary artery. Using the Design of Experiments and Response Surface methodologies, it was found for which values of D_1/D and α the dimensionless pressure drop $\tilde{p}$ was minimized. In all situations, as the diameter ratio increased to 1 and the junction angle decreased to 30º, $\tilde{p}$ decreased. Also, it was possible to notice a considerable dependence of $\tilde{p}$ on the stenosis degree *S*. The optimum point for all cases was $D_1/D_{,opt}$ equal to 1 and $\alpha_{,opt}$ equal to 30°, which was confirmed by previous studies. Besides, the results showed that D_1/D had more significant effects than α when the isolated effects on velocity contours and wall shear stress (WSS) were evaluated.

Chapter 3 applied the same methodology as Chapter 2 but investigated numerically the effects of rheological parameters in different flow conditions of the bypass graft. In this case, a comparison between the Newtonian and non-Newtonian results was done, and eighteen response surfaces were generated, each one representing the results for specific combinations of Carreau rheological parameters and Reynolds Number *Re*. All the response surfaces generated for both the Newtonian and non-Newtonian cases presented a great similarity. For the two Reynolds number here studied, the Newtonian case showed the lowest value of the dimensionless pressure drop, which can suggest that the choice of applying Newtonian blood may underestimate the value of pressure drop for the system. Even so, the results obtained demonstrated that non-Newtonian rheological parameters influenced neither the shape of the response surfaces nor the optimum points found. Besides that, the optimum point for all cases

was identical, i.e., $D_1/D_{,opt}$ equal to 1 and $\alpha_{,opt}$ equal to 30°. Finally, the rheological parameters, η^* and n, appear to have a more pronounced influence on velocity than λ.

The main conclusions and the optimal graft design found in this work are in accordance with previous Newtonian and non-Newtonian studies that evaluated the graft design with other methodologies. Therefore, starting from the outcomes obtained here, it is evident that the introduction of the Constructal Design method in the area of hemodynamics can provide valuable results for problems that literature still does not provide a definitive clarification.

The evaluation of pulsatile flow, the application to other bypass geometries, and the assumption of Fluid–Structure Interaction (FSI) are some suggestions for future works.

5 REFERENCES

ABRAHAM, F.; BEHR, M.; HEINKENSCHLOSS, M. Shape Optimization in Stationary Blood Flow: A Numerical Study of Non-Newtonian Effects. **Computer Methods in Biomechanics and Biomedical Engineering**, v. 8, p. 127–137, 2005. <http://dx.doi.org/10.1080/10255840500309562>

ANDERSSON, Magnus; EBBERS, Tino; KARLSSON, Matts. Characterization and estimation of turbulence-related wall shear stress in patient-specific pulsatile blood flow. **Journal of Biomechanics**, v. 85, p. 108–117, 2019. <https://doi.org/10.1016/j.jbiomech.2019.01.016>

ANSYS. **Ansys Fluent User's Guide**. Canonsburg, 2015.

ANSYS. **Design Xplorer User's Guide. Release 17.2**. Canonsburg, 2016.

APOSTOLIDIS, Alex J.; MOYER, Adam P.; BERIS, Antony N. Non-Newtonian effects in simulations of coronary arterial blood flow. **Journal of Non-Newtonian Fluid Mechanics**, v. 233, p. 155–165, 2016. <http://dx.doi.org/10.1016/j.jnnfm.2016.03.008>

BASSIOUNY, Hisham S.; WHITE, Scott; GLAGOV, Seymour; CHOI, Eric; GIDDENS, Don P.; ZARINS, Christopher K. Anastomotic intimal hyperplasia: Mechanical injury or flow induced. **Journal of Vascular Surgery**, v. 15, n. 4, p. 708–717, 1992. <https://doi.org/10.1067/mva.1992.33849>

BEJAN, A. **Advanced Engineering Thermodynamics**. 2 ed, Wiley, New York, 1997.

BEJAN, A; LORENTE, S. **Design with Constructal Theory**. Wiley, Hoboken, 2008.

BEJAN, A.; LORENTE, S. The constructal law and the evolution of design in nature. **Physics of Life Reviews**, v. 8, p. 209–240, 2011. <https://doi.org/10.1016/j.plrev.2011.05.010>

BEJAN, A.; ZANE, J. P. **Design in Nature: How the Constructal Law Governs Evolution in Physics**, Biology, Technology, and Social Organization. Doubleday, New York, 2012.

BEJAN, A. **The Physics of Life**, St. Martin's Press, New York, 2016.

BERTOLOTTI, C.; DEPLANO, V.; FUSERI, J.; DUPOUY, P. Numerical and experimental models of post-operative realistic flows in stenosed coronary bypasses. **Journal of Biomechanics**, v. 34, n. 8, p. 1049–1064, 2001. <https://doi.org/10.1016/S0021-9290(01)00027-6>

BERTOLOTTI, C; DEPLANO, V. Three-dimensional numerical simulations of flow through a stenosed coronary bypass. **Journal of Biomechanics**, v. 33, p. 1011–1022, 2000. <https://doi.org/10.1016/S0021-9290(00)00012-9>

BODNÁR, T.; SEQUEIRA, A.; PROSI, M. On the shear-thinning and viscoelastic effects of blood flow under various flow rates. **Applied Mathematics and Computation**, v. 217, n. 11, p. 5055–5067, 2011. <http://dx.doi.org/10.1016/j.amc.2010.07.054>

BRUN, Jean Frédéric; VARLET-MARIE, Emmanuelle; CASSAN, Delphine; RAYNAUD DE MAUVERGER, Eric. Blood rheology and body composition as determinants of exercise performance in female rugby players. **Clinical Hemorheology and Microcirculation**, v. 49, n. 1–4, p. 207–214, 2011. <http://dx.doi.org/10.3233/CH-2011-1470>

BRUN, Jean Frédéric; VARLET-MARIE, Emmanuelle; FÉDOU, Christine; RAYNAUD DE MAUVERGER, Eric. One-year follow-up of blood viscosity factors and hematocrit/viscosity ratio in elite soccer players. **Clinical Hemorheology and Microcirculation**, v. 64, n. 4, p. 799–808, 2016. <http://dx.doi.org/10.3233/CH-168014>

CARO, C. G.; FITZ-GERALD, J. M.; SCHROTER, R. C. Atheroma and arterial wall shear - Observation, correlation and proposal of a shear dependent mass transfer mechanism for atherogenesis. **Proceedings of the Royal Society of London. Series B. Biological Sciences**, v. 177, n. 1046, p. 109–159, 1971. <https://doi.org/10.1098/rspb.1971.0019>

CARREAU, Pierre J. Rheological Equations From Molecular Network Theories. **Transactions of the Society of Rheology**, v. 16, n. 1, p. 99–127, 1972. <https://doi.org/10.1122/1.549276>

CELIK, I. B.; GHIA, U.; ROACHE, P. J.; FREITAS, C. J.; COLEMAN, H.; RAAD, P. E. Procedure for Estimation and Reporting of Uncertainty Due to Discretization in CFD Applications. **Journal of Fluids Engineering**, v. 130, p. 128–131, 2008.

CHAICHANA, Thanapong; SUN, Zhonghua; JEWKES, James. Computation of hemodynamics in the left coronary artery with variable angulations. **Journal of Biomechanics**, v. 44, n. 10, p. 1869–1878, 2011. <http://dx.doi.org/10.1016/j.jbiomech.2011.04.033>

CHEN, Jie; LU, Xi Yun; WANG, Wen. Non-Newtonian effects of blood flow on hemodynamics in distal vascular graft anastomoses. **Journal of Biomechanics**, v. 39, n. 11, p. 1983–1995, 2006. <http://dx.doi.org/10.1016/j.jbiomech.2005.06.012>

CHEN, L. Progress in study on constructal theory and its applications. **Science China Technological Sciences**, v. 55, n. 3, p. 802–820, 2012. <https://doi.org/10.1007/s11431-011-4701-9>

CHO, Y. I.; KENSEY, K. R. Effects of the non-Newtonian viscosity of blood on flows in a diseased arterial vessel. Part 1: Steady flows. **Biorheology**, v. 28, n. 3–4, p. 241–262, 1991. <http://dx.doi.org/10.3233/BIR-1991-283-415>

CHUA, Leok Poh; TONG, Jia Hui; ZHOU, Tongming. Numerical simulation of steady flows in designed sleeve models at distal anastomoses. **International Communications in Heat and Mass Transfer**, v. 32, n. 5, p. 707–714, 2005. <http://dx.doi.org/10.1016/j.icheatmasstransfer.2004.08.025>

CHUA, Leok Poh; ZHANG, Junmei; ZHOU, Tongming. Numerical study of a complete anastomosis model for the coronary artery bypass. **International Communications in Heat and Mass Transfer**, v. 32, n. 3–4, p. 473–482, 2005. <http://dx.doi.org/10.1016/j.icheatmasstransfer.2004.03.016>

COLE, J. S.; WATTERSON, J. K.; O'REILLY, M. J. G. Numerical investigation of the haemodynamics at a patched arterial bypass anastomosis. **Medical Engineering and Physics**, v. 24, n. 6, p. 393–401, 2002. <https://doi.org/10.1016/S1350-4533(02)00038-3>

CONTI, Michele; LONG, Chris; MARCONI, Michele; BERCHIOLLI, Raffaella; BAZILEVS, Yuri; REALI, Alessandro. Carotid artery hemodynamics before and after stenting: A patient specific CFD study. **Computers and Fluids**, v. 141, p. 62–74, 2016. <http://dx.doi.org/10.1016/j.compfluid.2016.04.006>

DE SOUZA MENDES, Paulo R. Dimensionless non-Newtonian fluid mechanics. **Journal of Non-Newtonian Fluid Mechanics**, v. 147, n. 1–2, p. 109–116, 2007. <https://doi.org/10.1016/j.jnnfm.2007.07.010>

DO, Hung; OWIDA, Amal A.; YANG, William; MORSI, Yos S. Numerical simulation of the haemodynamics in end-to-side anastomoses. **International Journal for Numerical Methods in Fluids**, v. 67, p. 638–650, 2010. <http://dx.doi.org/10.1002/fld.2381>

DOOST, Siamak N.; ZHONG, Liang; SU, Boyang; MORSI, Yosry S. The numerical analysis of non-Newtonian blood flow in human patient-specific left ventricle. **Computer Methods and Programs in Biomedicine**, v. 127, p. 232–247, 2016. <http://dx.doi.org/10.1016/j.cmpb.2015.12.020>

DUTRA, R. F.; ZINANI, F. S. F.; ROCHA, L. A. O.; BISERNI, C. Constructal design of an arterial bypass graft**. Heat Transfer**, p. 1–21, 2020.<http://dx.doi.org/10.1002/htj.21693>

FAGUNDES, T. M.; LORENZINI, G.; ESTRADA, E. da S. D.; ISOLDI, L. A.; DOS SANTOS, E. D.; ROCHA, L. A. O.; DA SILVA NETO, A. J. Constructal Design of Conductive Asymmetric Tri-Forked Pathways. **Journal of Engineering Thermophysics**, v. 28, n. 1, p. 26–42, 2019. <http://dx.doi.org/10.1134/S181023281901003X>

FAN, Tingting; LU, Yuan; GAO, Yan; MENG, Jie; TAN, Wenchang; HUO, Yunlong; KASSAB, Ghassan S. Hemodynamics of left internal mammary artery bypass graft: Effect of anastomotic geometry, coronary artery stenosis, and postoperative time. **Journal of Biomechanics**, v. 49, n. 5, p. 645–652, 2016. <http://dx.doi.org/10.1016/j.jbiomech.2016.01.031>

FAN, Yubo; XU, Zaipin; JIANG, Wentao; DENG, Xiaoyan; WANG, Ke; SUN, Anqiang. An S-type bypass can improve the hemodynamics in the bypassed arteries and suppress intimal hyperplasia along the host artery floor. **Journal of Biomechanics**, v. 41, n. 11, p. 2498–2505, 2008. <http://dx.doi.org/10.1016/j.jbiomech.2008.05.008>

FORTUNY, Gerard; HERRERO, Joan; PUIGJANER, Dolors; OLIVÉ, Carme; MARIMON, Francesc; GARCIA-BENNETT, Josep; RODRÍGUEZ, Daniel. Effect of anticoagulant treatment in deep vein thrombosis: A patient-specific computational fluid dynamics study. **Journal of Biomechanics**, v. 48, n. 10, p. 2047–2053, 2015. <http://dx.doi.org/10.1016/j.jbiomech.2015.03.026>

GIJSEN, F. J. H.; ALLANIC, E.; VAN DE VOSSE, F. N.; JANSSEN, J. D. The influence of the non-Newtonian properties of blood on the flow in large arteries: Unsteady flow in a 90° curved tube. **Journal of Biomechanics**, v. 32, n. 7, p. 705–713, 1999. <http://dx.doi.org/10.1016/S0021-9290(99)00014-7>

GUERCIOTTI, Bruno; VERGARA, Christian; IPPOLITO, Sonia; QUARTERONI, Alfio; ANTONA, Carlo; SCROFANI, Roberto. A computational fluid–structure interaction analysis of coronary Y-grafts. **Medical Engineering and Physics**, v. 47, p. 117–127, 2017. <http://dx.doi.org/10.1016/j.medengphy.2017.05.008>

GUIRAUDOU, Marie; VARLET-MARIE, Emmanuelle; RAYNAUD DE MAUVERGER, Eric; BRUN, Jean Frédéric. Obesity-related increase in whole blood viscosity includes different profiles according to fat localization. **Clinical Hemorheology and Microcirculation**, v. 55, n. 1, p. 63–73, 2013. <http://dx.doi.org/10.3233/CH-131690>

HARUGUCHI, Hiroaki; TERAOKA, Satoshi. Intimal hyperplasia and hemodynamic factors in arterial bypass and arteriovenous grafts: A review. **Journal of Artificial Organs**, v. 6, n. 4, p. 227–235, 2003. <http://dx.doi.org/10.1007/s10047-003-0232-x>

HORNER, Jeffrey S.; ARMSTRONG, Matthew J.; WAGNER, Norman J.; BERIS, Antony N. Investigation of blood rheology under steady and unidirectional large amplitude oscillatory shear. **Journal of Rheology**, v. 62, n. 2, p. 577–591, 2018. <https://doi.org/10.1122/1.5017623>

IASIELLO, Marcello; VAFAI, Kambiz; ANDREOZZI, Assunta; BIANCO, Nicola. Analysis of non-Newtonian effects within an aorta-iliac bifurcation region. **Journal of Biomechanics**, v. 64, p. 153–163, 2017. <https://doi.org/10.1016/j.jbiomech.2017.09.042>

JOHNSTON, Barbara M.; JOHNSTON, Peter R.; CORNEY, Stuart; KILPATRICK, David. Non-Newtonian blood flow in human right coronary arteries: Steady state simulations. **Journal of Biomechanics**, v. 37, n. 5, p. 709–720, 2004. <http://dx.doi.org/10.1016/j.jbiomech.2003.09.016>

JOHNSTON, Barbara M.; JOHNSTON, Peter R.; CORNEY, Stuart; KILPATRICK, David. Non-Newtonian blood flow in human right coronary arteries: Transient simulations. **Journal of Biomechanics**, v. 39, n. 6, p. 1116–1128, 2006. <http://dx.doi.org/10.1016/j.jbiomech.2005.01.034>

KARIMI, Safoora; DABAGH, Mahsa; VASAVA, Paritosh; DADVAR, Mitra; DABIR, Bahram; JALALI, Payman. Effect of rheological models on the hemodynamics within human aorta: CFD study on CT image-based geometry. **Journal of Non-Newtonian Fluid Mechanics**, v. 207, p. 42–52, 2014. <http://dx.doi.org/10.1016/j.jnnfm.2014.03.007>

KIM, Ji Tae; SUNG, Kun Hyuk; RYOU, Hong Sun. A numerical study on the effect of hematocrit on hemodynamic characteristics in arteriovenous graft. **Korea Australia Rheology Journal**, v. 26, n. 3, p. 327–334, 2014. <http://dx.doi.org/10.1007/s13367-014-0037-x>

KO, T. H.; TING, K.; YEH, H. C. Numerical investigation on flow fields in partially stenosed artery with complete bypass graft: An in vitro study. **International Communications in Heat and Mass Transfer**, v. 34, n. 6, p. 713–727, 2007. <http://dx.doi.org/10.1016/j.icheatmasstransfer.2007.03.010>

KO, T. H.; TING, K.; YEH, H. C. A numerical study on the effects of anastomotic angle on the flow fields in a stenosed artery with a complete bypass graft. **International Communications in Heat and Mass Transfer**, v. 35, n. 10, p. 1360–1367, 2008. <http://dx.doi.org/10.1016/j.icheatmasstransfer.2008.06.010>

KU, David N; GIDDENS, Don P.; ZARINS, Christopher K.; GLAGOV, Seymour. Pulsatile Flow and Atherosclerosis in the Human Carotid Bifurcation. **Ateriosclerosis**, v. 5, p. 293–302, 1985. <https://doi.org/10.1161/01.ATV.5.3.293>

LEE, D.; SU, J. M.; LIANG, H. Y. A numerical simulation of steady flow fields in a bypass tube. **Journal of Biomechanics**, v. 34, n. 11, p. 1407–1416, 2001. <https://doi.org/10.1016/S0021-9290(01)00131-2>

LEI, M.; ARCHIE, J. P.; KLEINSTREUER, C. Computational design of a bypass graft that minimizes wall shear stress gradients in the region of the distal anastomosis. **Journal of Vascular Surgery**, v. 25, n. 4, p. 637–646, 1997. <https://doi.org/10.1016/S0741-5214(97)70289-1>

LEUPRECHT, Armin; PERKTOLD, Karl; PROSI, Martin; BERK, Thomas; TRUBEL, Wolfgang; SCHIMA, Heinrich. Numerical study of hemodynamics and wall mechanics in distal end-to-side anastomoses of bypass grafts. **Journal of Biomechanics**, v. 35, n. 2, p. 225–236, 2002. <https://doi.org/10.1016/S0021-9290(01)00194-4>

LIU, Guiying; WU, Jianhuang; GHISTA, Dhanjoo N.; HUANG, Wenhua; WONG, Kelvin K. L. Hemodynamic characterization of transient blood flow in right coronary arteries with varying curvature and side-branch bifurcation angles. **Computers in Biology and Medicine**, v. 64, p. 117–126, 2015. <http://dx.doi.org/10.1016/j.compbiomed.2015.06.009>

LIU, Xiao; WANG, Libing; WANG, Zhenze; LI, Zhengxing; KANG, Hongyan; FAN, Yubo; SUN, Anqiang; DENG, Xiaoyan. Bioinspired helical graft with taper to enhance helical flow. **Journal of Biomechanics**, v. 49, n. 15, p. 3643–3650, 2016. <http://dx.doi.org/10.1016/j.jbiomech.2016.09.028>

LUCIA, Umberto; GRISOLIA, Giulia; DOLCINO, Daniela; ASTORI, Maria Rosa; MASSA, Eugenio; PONZETTO, Antonio. Constructal approach to bio-engineering: the ocular anterior chamber temperature. **Scientific Reports**, v. 6, p. 1–6, 2016. <http://dx.doi.org/10.1038/srep31099>

LUCIA, Umberto; GRISOLIA, Giulia; ASTORI, Maria Rosa. Constructal law analysis of Cl^- transport in eyes aqueous humor. **Scientific Reports**, v. 7, n. 1, p. 8–11, 2017. <http://dx.doi.org/10.1038/s41598-017-07357-8>

LUCIA, Umberto; GRISOLIA, Giulia. Constructal law and ion transfer in normal and cancer cells. **Proceedings of the Romanian Academy**, Series A, v. 19, Special Issue, p. 213–218, 2018. <https://academiaromana.ro/sectii2002/proceedings/doc2018-1s/continut/213-218.pdf>

MARCINKOWSKA-GAPIŃSKA, Anna; GAPINSKI, Jacek; ELIKOWSKI, Waldemar; JAROSZYK, Feliks; KUBISZ, Leszek. Comparison of three rheological models of shear flow behavior studied on blood samples from post-infarction patients. **Medical and Biological Engineering and Computing**, v. 45, n. 9, p. 837–844, 2007. <http://dx.doi.org/10.1007/s11517-007-0236-4>

MEHRI, Rym; MAVRIPLIS, Catherine; FENECH, Marianne. Red blood cell aggregates and their effect on non-Newtonian blood viscosity at low hematocrit in a two-fluid low shear rate microfluidic system. **PLoS ONE**, v. 13, n. 7, 2018. <http://dx.doi.org/10.1371/journal.pone.0199911>

MOLLA, M. M.; PAUL, M. C. LES of non-Newtonian physiological blood flow in a model of arterial stenosis. **Medical Engineering and Physics**, v. 34, n. 8, p. 1079–1087, 2012. <https://doi.org/10.1016/j.medengphy.2011.11.013 >

MONTGOMERY, D.C. **Design and Analysis of Experiments**, 8. ed., John Wiley & Sons, New Jersey, 2013.

O'CALLAGHAN, Siobhan; WALSH, Michael; MCGLOUGHLIN, Timothy. Numerical modelling of Newtonian and non-Newtonian representation of blood in a distal end-to-side vascular bypass graft anastomosis. **Medical Engineering and Physics**, v. 28, p. 70–74, 2006. <http://dx.doi.org/10.1016/j.medengphy.2005.04.001>

OJHA, Matadial; CORMIER, Jean M.; COBBOLD, Richard S. C. Hemodynamics of a side-to-end proximal arterial anastomosis model. **Journal of Vascular Surgery**, v. 17, n. 4, p. 646–655, 1993. <https://doi.org/10.1067/mva.1993.39516>

OJHA, Matadial. Wall Shear Stress Temporal Gradient and Anastomotic Intimal Hyperplasia. **Circulation Research**, v. 74, p. 1227–1231, 1994. <https://doi.org/10.1161/01.res.74.6.1227>

OWENS, Robert G. A new microstructure-based constitutive model for human blood. **Journal of Non-Newtonian Fluid Mechanics**, v. 140, n. 1–3, p. 57–70, 2006. <http://dx.doi.org/10.1016/j.jnnfm.2006.01.015>

OWIDA, Amal Ahmed; DO, Hung; MORSI, Yos S. Numerical analysis of coronary artery bypass grafts: An over view. **Computer Methods and Programs in Biomedicine**, v. 108, n. 2, p. 689–705, 2012. <http://dx.doi.org/10.1016/j.cmpb.2011.12.005>

PATANKAR, S. V. **Numerical Heat Transfer and Fluid Flow**. McGraw-Hill, New York, 1980.

PEIFFER, Veronique; SHERWIN, Spencer J.; WEINBERG, Peter D. Does low and oscillatory wall shear stress correlate spatially with early atherosclerosis? A systematic review. **Cardiovascular Research**, v. 99, n. 2, p. 242–250, 2013. <https://doi.org/10.1093/cvr/cvt044>

PEREIRA, J. M. C.; SERRA E MOURA, J.P.; ERVILHA, A.R.; PEREIRA, J.C.F. On the uncertainty quantification of blood flow viscosity models. **Chemical Engineering Science**, v. 101, p. 253–265, 2013. <http://dx.doi.org/10.1016/j.ces.2013.05.033>

POLITIS, A. K.; STAVROPOULOS, G. P.; CHRISTOLIS, M. N.; PANAGOPOULOS, F. G.; VLACHOS, N. S.; MARKATOS, N. C. Numerical modeling of simulated blood flow in idealized composite arterial coronary grafts: Steady state simulations. **Journal of Biomechanics**, v. 40, n. 5, p. 1125–1136, 2007.
<https://doi.org/10.1016/j.jbiomech.2006.05.008>

POST, Allison; DIAZ-RODRIGUEZ, Patricia; BALOUCH, Bailey; PAULSEN, Samantha; WU, Siliang; MILLER, Jordan; HAHN, Mariah; COSGRIFF-HERNANDEZ, Elizabeth. Elucidating the role of graft compliance mismatch on intimal hyperplasia using an ex vivo organ culture model. **Acta Biomaterialia**, v. 89, p. 84–94, 2019.
<https://doi.org/10.1016/j.actbio.2019.03.025>

RAZAVI, A.; SHIRANI, E.; SADEGHI, M. R. Numerical simulation of blood pulsatile flow in a stenosed carotid artery using different rheological models. **Journal of Biomechanics**, v. 44, n. 11, p. 2021–2030, 2011. <http://dx.doi.org/10.1016/j.jbiomech.2011.04.023>

RAZERA, A. L.; DA FONSECA, R. J. C.; ISOLDI, L. A.; DOS SANTOS, E. D.; ROCHA, L. A. O.; BISERNI, C. Constructal design of a semi-elliptical fin inserted in a lid-driven square cavity with mixed convection. **International Journal of Heat and Mass Transfer**, v. 126, p. 81–94, 2018. <https://doi.org/10.1016/j.ijheatmasstransfer.2018.05.157>

REIS, A. H. Constructal theory: from engineering to physics, and how flow systems develop shape and structure. **Applied Mechanics Reviews**, v. 59, p. 269–282, 2006.
<https://doi.org/10.1115/1.2204075>

ROCHA, L. A. O.; LORENTE, S.; BEJAN, A. Constructal Theory in Heat Transfer. In: KULACKI F. **Handbook of Thermal Science and Engineering.** Springer, 2017. Chap. 1, p. 1-32. <https://doi.org/10.1007/978-3-319-32003-8_66-1>

ROOS, M. W.; WADBRO, E.; BERGGREN, M. Computational estimation of fluid mechanical benefits from a fluid deflector at the distal end of artificial vascular grafts. **Computers in Biology and Medicine**, v. 43, n. 2, p. 164–168, 2013.
<http://dx.doi.org/10.1016/j.compbiomed.2012.11.012>

SLATTERY, J., C. **Advanced Transport Phenomena**. Cambridge University Press, New York, 1999.

SOOD, Tapan; ROY, Somnath; PATHAK, Manabendra. Effect of pulse rate variation on blood flow through axisymmetric and asymmetric stenotic artery models. **Mathematical Biosciences**, v. 298, n. February, p. 1–18, 2018.
<https://doi.org/10.1016/j.mbs.2018.01.008>

TIAN, Fang Bao; ZHU, Luoding; FOK, Pak Wing; LU, Xi Yun. Simulation of a pulsatile non-Newtonian flow past a stenosed 2D artery with atherosclerosis. **Computers in Biology and Medicine**, v. 43, n. 9, p. 1098–1113, 2013.
<https://doi.org/10.1016/j.compbiomed.2013.05.023>

TSUKUI, Hiroyuki; SHINKE, Manabu; PARK, Young Kwang; YAMAZAKI, Kenji. Longer coronary anastomosis provides lower energy loss in coronary artery bypass grafting. **Heart and Vessels**, v.32, n. 1, p. 83–89, 2017. <http://dx.doi.org/10.1007/s00380-016-0880-4>

VIMMR, Jan; JONÁŠOVÁ, Alena. Non-Newtonian effects of blood flow in complete coronary and femoral bypasses. **Mathematics and Computers in Simulation**, v. 80, n. 6, p. 1324–1336, 2010. <https://doi.org/10.1016/j.matcom.2009.01.004>

VIMMR, Jan; JONÁŠOVÁ, Alena; BUBLÍK, Ondřej. Effects of three geometrical parameters on pulsatile blood flow in complete idealised coronary bypasses. **Computers and Fluids**, v. 69, p. 147–171, 2012. <https://doi.org/10.1016/j.compfluid.2012.08.007>

VIMMR, J.; JONÁŠOVÁ, A.; BUBLÍK, O. Numerical analysis of non-Newtonian blood flow and wall shear stress in realistic single, double and triple aorto-coronary bypasses. **International Journal for Numerical Methods in Biomedical Engineering**, v. 29, p. 1057–1081, 2013. <http://dx.doi.org/10.1002/cnm.2560>

WANG, Haojie; DAI, Weizhong; BEJAN, Adrian. Optimal temperature distribution in a 3D triple-layered skin structure embedded with artery and vein vasculature and induced by electromagnetic radiation. **International Journal of Heat and Mass Transfer**, v. 50, p. 1843–1854, 2007. <http://dx.doi.org/10.1016/j.ijheatmasstransfer.2006.10.005>

WEDDELL, Jared C; KWACK, JaeHyuk; IMOUKHUEDE, P. I.; MASUD, Arif. Hemodynamic analysis in an idealized artery tree: Differences in wall shear stress between Newtonian and non-Newtonian blood models. **PLoS ONE**, v. 10, n. 4, p. 1–23, 2015. <http://dx.doi.org/10.1371/journal.pone.0124575>

XIONG, F. L.; CHONG, C. K. A parametric numerical investigation on haemodynamics in distal coronary anastomoses. **Medical Engineering and Physics**, v. 30, n. 3, p. 311–320, 2008. <https://doi.org/10.1016/j.medengphy.2007.04.013>

ZINANI, Flávia; FREY, Sérgio. Galerkin least-squares multifield approximations for flows of inelastic non-Newtonian fluids. **Journal of Fluids Engineering**, v. 130, n. 8, p. 081507 1–14, 2008. <https://doi.org/10.1115/1.2956514>

ZYDNEY, A. L.; OLIVER, J. D.; COLTON, C. K. A constitutive equation for the viscosity of stored red cell suspensions: Effect of hematocrit, shear rate, and suspending phase. **Journal of Rheology**, v. 35, n. 8, p. 1639–1680, 1991. <http://dx.doi.org/10.1122/1.550249>